

Non-Abelian Majorana Doublets in Time-Reversal Invariant Topological Superconductor

Xiong-Jun Liu,^{1,2} Chris L. M. Wong,¹ and K. T. Law¹

¹*Department of Physics, Hong Kong University of Science and Technology, Clear Water Bay, Hong Kong, China*

²*Institute for Advanced Study, Hong Kong University of Science and Technology, Clear Water Bay, Hong Kong, China*
(Dated: April 16, 2013)

The study of non-Abelian Majorana zero modes advances our understanding of the fundamental physics in quantum matter, and pushes their potential applications to topological quantum computation. Recent investigations have shown that in the two-dimensional (2D) and 1D chiral superconductors, braiding isolated Majorana zero modes leads to noncommutative transformation of the quantum states [1, 2]. However, Majorana fermions in a Z_2 time-reversal invariant (TRI) topological superconductor come in pairs due to Kramers' theorem [3]. Therefore, braiding operations in TRI superconductors always exchange two pairs of Majorana fermions. In this work, we show surprisingly that, due to the protection of time-reversal symmetry, non-Abelian statistics can be obtained in the 1D TRI topological superconductor and may have advantages in applying to topological quantum computation. Furthermore, we predict a novel phenomenon in the Josephson effect for 1D TRI topological superconductors, which measures the topological qubit states in such systems.

The search for exotic non-Abelian quasiparticles has been a focus of both theoretical and experimental studies in condensed matter physics, driven largely by their promising applications to fault-tolerant topological quantum computation [4–9]. Following this pursuit, the topological superconductors have been brought to the forefront for they host exotic zero energy states known as Majorana fermions [10–15]. For 2D chiral $p + ip$ pairing state, which breaks time-reversal symmetry, one Majorana mode exists in each vortex core [5], and for 1D p -wave case, such state locates at each end of the system [6]. Existence of $2n$ Majorana zero modes leads to 2^{n-1} -fold ground-state degeneracy, and braiding two of such modes transforms one state into another which defines the non-Abelian statistics [1, 2]. Remarkably, Majorana end states have been suggestively observed through tunneling measurements [16] in 1D effective p -wave superconductors obtained by semiconductor nanowire/ s -wave superconductor heterostructures [17–19].

Recently, a new class of topological superconductors with time-reversal symmetry, referred to as DIII symmetry class superconductor and classified by Z_2 topological invariant [3, 20–23], have attracted rapidly growing efforts [24–28]. Different from chiral superconductors, in DIII class superconductor the zero modes come in pairs due to Kramers' theorem. Several interesting proposals

have been studied to realize Z_2 TRI Majorana quantum wires using proximity effects of d -wave, p -wave or $s \pm$ -wave superconductors. It was shown that at each end of such a quantum wire are localized two Majorana fermions which form a Kramers doublet and are protected by time-reversal symmetry [26–28].

With the practicability in realization, a fundamental question is that can the DIII class topological superconductor be applied to topological quantum computation? The puzzle arises from the fact that braiding the end states in a DIII class 1D superconductor always exchanges two pairs of Majorana modes as illustrated in Fig. 1. While braiding two pairs of Majoranas in chiral topological superconductors yields Abelian operations, in this work, we show that braiding Majorana end states in DIII class superconductors is non-Abelian due to the protection by time-reversal symmetry.

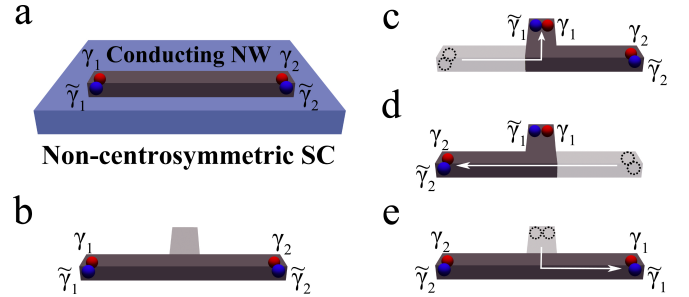


FIG. 1: Braiding Majorana zero modes in 1D TRI topological superconductor through a T-junction following the study by Alicea and the colleagues [2]. **a**, The DIII class topological superconductor can be realized by depositing a conducting nanowire (NW) on the top of a non-centrosymmetric superconductor (SC). **b-e**, Braiding end modes through a T-junction. The dark (light gray) area of the nanowires depicts the topological (trivial) region, which is controllable by tuning the chemical potential in the nanowire. The arrows depict the direction that the Majorana fermions are transported to in the braiding process.

In the Methods section, we show that a 1D TRI topological superconductor can be engineered by inducing p -wave superconductivity in a conducting wire in proximity to a non-centrosymmetric superconductor (Fig. 1a) [29]. In the topological phase, at each end of the wire are localized two Majorana zero modes γ_j and $\tilde{\gamma}_j$ ($j = 1, 2$), transformed by time-reversal operator that $\mathcal{T}^{-1}\gamma_j\mathcal{T} = \tilde{\gamma}_j$ and $\mathcal{T}^{-1}\tilde{\gamma}_j\mathcal{T} = -\gamma_j$ [20]. Note that braiding Majorana end modes is not well-defined for a single 1D nanowire and, as

first recognized by Alicea et al., the minimum setup for braiding requires a trijunction, e.g. a T-junction composed of two nanowire segments [2]. The braiding can be performed by transporting the Majorana zero modes following the steps as illustrated in Fig. 1(b-e).

To visualize the braiding rule, let us consider first the simplest situation that the DIII class topological superconductor is composed of two decoupled copies (e.g. corresponding to spin-up and spin-down, respectively) of 1D chiral p -wave superconductors. It is then straightforward to know that the whole braiding is a product of two independent processes of braiding $\gamma_{1,2}$ and $\tilde{\gamma}_{1,2}$, respectively, which gives the TRI unitary transformation matrix $U_{12}(T, \tilde{T}) = \exp(\frac{\pi}{4}\gamma_1\gamma_2)\exp(\frac{\pi}{4}\tilde{\gamma}_1\tilde{\gamma}_2)$ following the studies by Ivanov, Alicea and the colleagues [1, 2]. This braiding is nontrivial as presented below, and detailed in the Supplementary Material. We consider two DIII class wires with eight Majorana modes $\gamma_{1,\dots,4}$ and $\tilde{\gamma}_{1,\dots,4}$ (Fig. 2a), which define four complex fermion modes by $f_1 = \frac{1}{2}(\gamma_1 + i\gamma_2)$, $f_2 = \frac{1}{2}(\gamma_3 + i\gamma_4)$, and $\tilde{f}_{1,2} = \mathcal{T}^{-1}f_{1,2}\mathcal{T}$. The Hilbert space of the four complex fermions is spanned by sixteen qubit states $|n_1n_2\rangle|\tilde{n}_1\tilde{n}_2\rangle = (f_1^\dagger)^{n_1}(f_2^\dagger)^{n_2}(\tilde{f}_1^\dagger)^{\tilde{n}_1}(\tilde{f}_2^\dagger)^{\tilde{n}_2}|00\rangle|\tilde{0}\tilde{0}\rangle$. If the initial state of the system is $|00\rangle_L|00\rangle_R$, for instance, by braiding the two pairs of Majoranas $\gamma_2, \tilde{\gamma}_2$ and $\gamma_3, \tilde{\gamma}_3$ we get straightforwardly

$$U_{23}(T, \tilde{T})|0\tilde{0}\rangle_L|0\tilde{0}\rangle_R = \frac{1}{2}(|0\tilde{0}\rangle_L|0\tilde{0}\rangle_R + |1\tilde{1}\rangle_L|1\tilde{1}\rangle_R + i|1\tilde{0}\rangle_L|1\tilde{0}\rangle_R - i|0\tilde{1}\rangle_L|0\tilde{1}\rangle_R)(1)$$

Here L/R represents the left/right nanowire segment. It is interesting that the above state is generically a four-particle entangled state, which shows the natural advantage in generating multi-particle entangled state using DIII class topological superconductors. Furthermore, a full braiding, i.e. braiding twice $\gamma_2, \tilde{\gamma}_2$ and $\gamma_3, \tilde{\gamma}_3$ yields the final state $|1\tilde{1}\rangle_L|1\tilde{1}\rangle_R$, which distinguishes from the initial state in that each copy of the p -wave superconductor changes fermion parity.

From the above discussion we find that in the braiding the Majorana modes γ_j do not feel their time-reversal partners $\tilde{\gamma}_j$, which is an essential difference from the situation in exchanging two pairs of Majorana fermions in a chiral superconductor, and makes the braiding operator in a TRI topological superconductor nontrivial (Fig. 2b-c). As presented below, the above braiding statistics, while being obtained in the special situation, are valid in the generic DIII class 1D topological superconductors and protected by time-reversal symmetry.

We first prove a central result that by grouping all the quasiparticle states into two sectors being time-reversed partners of each other, the fermion parity is conserved for each sector, not only for the total system. The proof is equivalent to showing that in a TRI Majorana quantum wire, the four topological qubit states $|n_1\tilde{n}_1\rangle$ ($n_1, \tilde{n}_1 = 0, 1$) are decoupled from each other with the presence of finite TRI perturbations. The coupling

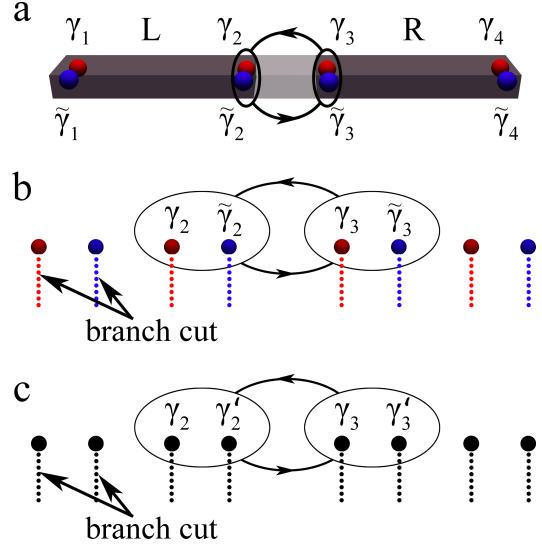


FIG. 2: **Non-Abelian statistics in DIII class 1D topological superconductor.** **a**, Majorana end modes $\gamma_2, \tilde{\gamma}_2$ and $\gamma_3, \tilde{\gamma}_3$ are braided through similar processes shown in Fig. 1. **b**, Braiding Majorana modes in DIII class superconductor is equivalent to two independent processes of exchanging γ_2, γ_3 and $\tilde{\gamma}_2, \tilde{\gamma}_3$, respectively. In the depicted process γ_2 ($\tilde{\gamma}_2$) crosses only the branch cut of γ_3 ($\tilde{\gamma}_3$), and therefore acquires a minus sign after braiding. **c**, In contrast, if braiding two Majorana pairs in a chiral superconductor, for the depicted process γ_2 (γ'_2) crosses the branch cuts of both γ_3 and γ'_3 , and then no sign change occurs after braiding [1]. Therefore, braiding twice two Majorana pairs always returns to the original state.

Hamiltonian, assumed to depend on a manipulatable parameter λ , should take the generic TRI form $V(\lambda) = iE_1(\lambda)(\gamma_1\gamma_2 - \tilde{\gamma}_1\tilde{\gamma}_2) + iE_2(\lambda)(\gamma_1\tilde{\gamma}_2 - \gamma_2\tilde{\gamma}_1)$, which splits the two even parity eigenstates $|00\rangle$ and $|11\rangle$ by an energy $E(\lambda) = 2\sqrt{E_1^2 + E_2^2}$. Since $|1\tilde{0}\rangle$ and $|0\tilde{1}\rangle$ form a Kramers' doublet, the transition between them is forbidden by time-reversal symmetry. Then the fermion parity conservation requires that the following adiabatic condition be satisfied in the manipulation: $|\langle 1\tilde{1}|\dot{\lambda}\partial_\lambda|0\tilde{0}\rangle| \ll 2E(\lambda)$, where $\dot{\lambda} = \partial\lambda/\partial t$. This is followed by

$$\tilde{R} \equiv \frac{1}{2E(\lambda)} \left| \frac{\partial\lambda}{\partial t} \frac{\partial\theta}{\partial\lambda} \right| \ll 1, \quad \theta = \tan^{-1} \frac{E_1}{E_2} \quad (2)$$

In a realistic system, the coupling $E_{1,2}$ are controlled by adjusting the bulk gap E_{bulk} or the distance d between the Majorana modes, and are generically exponential functions of $E_{\text{bulk}}d$. Since γ_j and $\tilde{\gamma}_j$ are connected by \mathcal{T} -transformation, their wave functions have exactly the same spatial profile, which leads to the same exponential form of the couplings $E_{1,2}(\lambda) = \alpha_{1,2}(\lambda)e^{-\beta E_{\text{bulk}}d}$. The pre-factors $\alpha_j(\lambda)$ depend on the local couplings (e.g. hopping terms, pairings, etc.) between electrons belonging to the same (for $j = 1$) or different (for $j = 2$) sectors of the time-reversal partners. For constant and homogeneous local couplings, we expect that while the magnitudes of $\alpha_j(\lambda)$ depend on λ , their ratio α_1/α_2 is nearly a

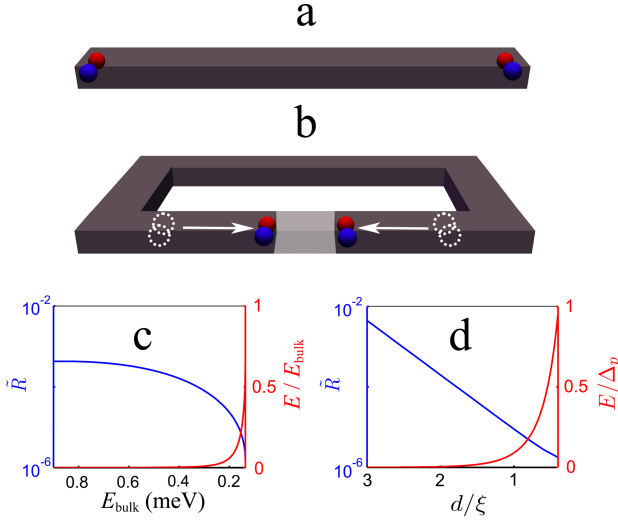


FIG. 3: **Adiabatic condition and fermion parity conservation for each sector of time-reversal partners.** **a-b**, The couplings $E_{1,2}$ between Majorana end modes are manipulated by tuning the chemical which changes the bulk gap ($\lambda = E_{\text{bulk}}$) in the nanowire (**a**), and by varying the length ($\lambda = d$) of a trivial region (gray color) which separates the two pairs of Majorana modes (**b**). **c-d**, The energy splitting E between $|0\tilde{0}\rangle$ and $|1\tilde{1}\rangle$ (red curves) and the ratio \tilde{R} (blue curves), as functions of E_{bulk} (**c**), and versus the trivial region distance d (**d**). The parameters in the nanowire are taken that the proximity induced p -wave pairing $\Delta_p = 1.0\text{meV}$, s -wave pairing $\Delta_s = 0.5\text{meV}$, and the spin-orbit coupling energy $E_{\text{so}} = 0.1\text{meV}$. In the numerical simulation we assume that the coupling energy E is tuned from 0 to 1.0meV in the time $1.0\mu\text{s}$. We also numerically confirmed the adiabatic condition $\tilde{R} \ll 1$ with other different parameter regimes.

constant (rigorous proof is given in Supplementary Material). Therefore we always have $\partial_\lambda \theta \approx 0$, which validates the adiabatic condition. This general statement is clearly shown with numerical results in Fig. 3. The fermion parity conservation for each sector shows that an isolated DIII class 1D Majorana wire should stay in one of the four fermion parity eigenstates germinated by non-local complex fermion operators f_j and \tilde{f}_j , given that time-reversal symmetry is not broken. In particular, one can always prepare a nanowire initially in the ground state $|0\tilde{0}\rangle$ or $|1\tilde{1}\rangle$ by controlling the initial couplings $E_{1,2}(\lambda)$, and then manipulate the states adiabatically.

The fermion parity conservation for each sector implies that the exchange of Majorana end modes in DIII class superconductor is generically equivalent to two independent processes of braiding Majorana fermions of two different sectors, respectively. This is because, first of all, braiding adiabatically the Majorana zero modes, e.g. $\gamma_1, \tilde{\gamma}_1$ and $\gamma_2, \tilde{\gamma}_2$, does not affect the bulk states which are gapped. Furthermore, assuming that other Majorana zero modes are located far away from $\gamma_{1,2}$ and $\tilde{\gamma}_{1,2}$, the braiding evolves only the Majorana modes which are exchanged. Finally, due to the fermion parity conser-

vation, in the braiding the fermion modes f_1 and \tilde{f}_1 are always decoupled and their dynamics can be derived independently. We therefore obtain the braiding matrix by $U_{12}(T, \tilde{T}) = \exp(\frac{\pi}{4}\gamma_1\gamma_2)\exp(\frac{\pi}{4}\tilde{\gamma}_1\tilde{\gamma}_2)$, as presented above. A rigorous derivative of the braiding matrix is given in the Supplementary Material.

It is important to study how to detect the topological qubit states in a DIII class Majorana quantum wire. We consider a Josephson junction shown in Fig. 4a formed by DIII class superconductor. As derived in the Supplementary Material, the effective coupling Hamiltonian of the Josephson junction is given by

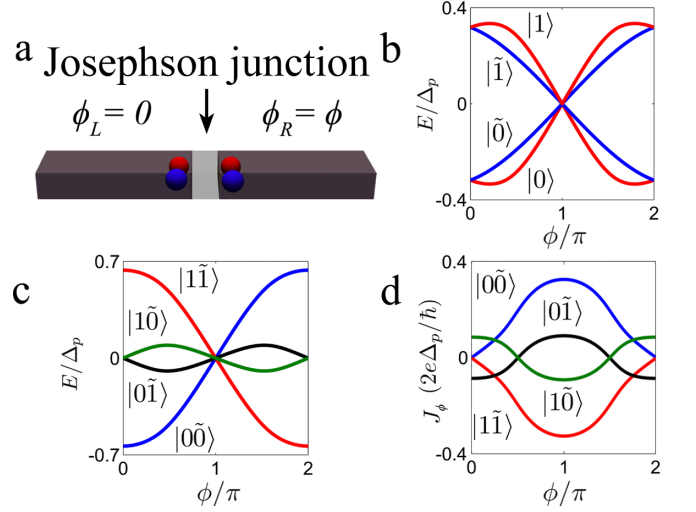


FIG. 4: **Josephson measurement of the topological qubit states in DIII class 1D topological superconductor.** **a**, The sketch of a Josephson junction with phase difference ϕ . **b**, The single particle Andreev bound state spectra versus the phase difference ϕ . **c**, The energy spectra of the four qubit states $|n_1\tilde{n}_1\rangle$ ($n_1, \tilde{n}_1 = 0, 1$) according to the results in **b**. **d**, The Josephson currents (in units of $2e\Delta_p/\hbar$) for different topological qubit states. Parameters used in the numerical calculation are taken that $\Delta_p = 1.0\text{meV}$, $\Delta_s = 0.25\text{meV}$, $E_{\text{so}} = 0.1\text{meV}$, the width of the junction $d = 0.5\xi$, and in middle trivial region (gray color) of the junction the chemical potential is set to be at the band bottom.

$$H_{\text{eff}} = i\Gamma_0 \cos \frac{\phi}{2} (\gamma_1\gamma_2 - \tilde{\gamma}_1\tilde{\gamma}_2) + i\Gamma_1 \sin \phi (\gamma_1\tilde{\gamma}_1 - \gamma_2\tilde{\gamma}_2) \quad (3)$$

where ϕ is the phase difference across the junction. The Γ_0 -term in H_{eff} represents the first-order direct coupling between Majorana fermions at different junction leads. The Γ_1 -term is resulted from the second-order perturbation of the tunneling process, and this term vanishes if the s -wave pairing $\Delta_s = 0$ (a detailed discussion can be found in the Supplementary Material). Redefining the Majorana bases by $\gamma'_1 = \gamma_1 + \tilde{\gamma}_2$ and $\gamma'_2 = \gamma_2 + \tilde{\gamma}_1$, we recast the above Hamiltonian into $H_{\text{eff}} = i(\Gamma_0 \cos \phi/2 + \Gamma_1 \sin \phi)\gamma'_1\gamma'_2 - i(\Gamma_0 \cos \phi/2 - \Gamma_1 \sin \phi)\tilde{\gamma}'_1\tilde{\gamma}'_2$, which gives straightforwardly the Andreev bound state spectra. Numerical results are shown in Fig. 4b-c. The Josephson

currents are obtained by the slope of the Andreev bound state spectra. In particular, we have that the Josephson currents $J_\phi^{\text{even}} = \pm \frac{e}{\hbar} \Gamma_0 \sin \frac{\phi}{2}$ for the even parity states, $|0\tilde{0}\rangle$ and $|1\tilde{1}\rangle$, and $J_\phi^{\text{odd}} = \pm \frac{e}{\hbar} \Gamma_1 \cos \phi$ for the odd parity states, $|0\tilde{1}\rangle$ and $|1\tilde{0}\rangle$, respectively (Fig. 4d).

Interestingly, the currents for odd-parity states are of 2π periodicity, half of those for even-parity states (Fig. 4d). This reflects that J_ϕ^{even} is contributed from the direct Majorana coupling induced by first-order tunneling, while J_ϕ^{odd} is a consequence of the second-order tunneling process which corresponds to the Cooper pair tunneling. Such result is also consistent with the fact that the time-reversal symmetry is restored with $|0\tilde{1}\rangle$ and $|1\tilde{0}\rangle$ forming Kramers' doublet at $\phi = m\pi$, which necessitates the 2π periodicity in their spectra. Furthermore, the two qubit states with the same total parity (e.g. $|0\tilde{0}\rangle$ and $|1\tilde{1}\rangle$) are distinguished by the direction of the currents. The qualitative difference in the Josephson currents provides direct measurements of the four topological qubit states in the experiment.

Methods

Topological superconductor of DIII class by proximity effect. Several interesting proposals have been studied for realizing DIII class 1D topological superconductor [26–28]. Here we consider to engineer such topological superconductor by depositing a conducting quantum wire on a non-centrosymmetric superconductor (Fig. 1). Details of the proximity effect are given in the Supplementary Material. The induced s - and p -wave superconductivity in the wire can be obtained by integrating out the degree of freedom of the superconductor substrate. This gives the spectral function of the wire

$$A(\omega, k_x) = -\frac{1}{2\pi} \Im \{ \text{tr} [\tau_z G_{\text{wire}}(\omega + i0^+, k_x)] \}$$

where $G_{\text{wire}}^{-1}(\omega, k_x) = \omega I - \xi_{k_x} \tau_z - \Sigma(\omega, k_x)$ is the Green's function of the wire. The induced s - and p -wave pairings, Δ_s and Δ_p , are encoded in the self-energy $\Sigma(\omega, k_x) = |t_\perp|^2 \int dk_y [\omega - H_{\text{SC}}(k_x, k_y)]^{-1}$ due to the coupling to the bulk superconductor with its Hamiltonian denoted by H_{SC} . Here t_\perp characterizes the coupling between the nanowire and substrate superconductor through their interface. The spectral function determines the effective Hamiltonian and the band structure of the wire. In the Supplementary Material we find that the nanowire is in the topological regime when its chemical potential μ the induced pairings satisfy $-2t_w < \mu < 2t_w$ and

$|\Delta_p| > |\Delta_s|$, where t_w denotes the hopping coefficient in the nanowire.

Non-Abelian braiding. To realize a DIII class superconductor applies no external magnetic field, which can be advantageous to construct realistic Majorana network to implement braiding operations. In comparison, for the chiral topological superconductor observed in a spin-orbit coupled semiconductor nanowire using s -wave superconducting proximity effect [17–19], the external magnetic field should be applied perpendicular to the spin quantization axis by spin-orbit interaction, driving optimally the nanowire into topological phase [17, 19, 30]. It is shown that for a network formed by multiple nanowire segments, such optimal condition cannot be reached for all segments without inducing detrimental orbital effects, which creates further experimental challenges in braiding Majoranas [30]. It is clear that such intrinsic difficulty is absent in the present DIII class TRI topological superconductor, and one may have more flexibility in constructing 2D and even 3D Majorana networks for topological quantum computation.

Josephson effect in DIII class topological superconductor. After braiding the end modes, we can transport the Majorana modes to the Josephson junction and measure the topological qubit states by Josephson effect. It turns out that the first-order direct coupling occurs only between Majorana modes at different ends of the junction, yielding the first term in the coupling Hamiltonian H_{eff} of Eq. (3). The leading-order contribution to the coupling between Majorana fermions at the same end ($i\gamma_j \tilde{\gamma}_j$) comes from the second-order perturbation in the tunneling process. This is because, the coupling term such as $i\gamma_j \tilde{\gamma}_j$ breaks time-reversal symmetry, while the direct coupling between γ_j and $\tilde{\gamma}_j$ does not experience the phase difference across the junction and therefore should preserve time-reversal symmetry. To get the second term in H_{eff} , the minimum requirement is to consider the second-order tunneling process. Furthermore, since the system restores time-reversal symmetry at $\phi = m\pi$, the leading-order contribution to $i\gamma_j \tilde{\gamma}_j$ must be proportional to $\sin \phi$, which has 2π periodicity. These properties are unaffected by TRI disorder scattering.

Acknowledgement

We appreciate the very helpful discussions with P. A. Lee, L. Fu, Z.-X. Liu, A. Potter, Z. -C. Gu, M. Cheng, and X. G. Wen. The authors thank the support of HKRGC through DAG12SC01, Grant 605512, and HKUST3/CRF09.

-
- [1] Ivanov, D. A. Non-Abelian statistics of half-quantum vortices in p -wave superconductors. *Phys. Rev. Lett.* **86**, 268-271 (2001).
 [2] Alicea, J., Oreg, Y., Refael, G., von Oppen, F. & Fisher,

- M. P. A. Non-Abelian statistics and topological quantum information processing in 1D wire networks. *Nature Phys.* **7**, 412-417 (2011).
 [3] Schnyder, A. P., Ryu, S., Furusaki, A. & Ludwig, A. W.

- W. Topological insulators and superconductors: ten-fold way and dimensional hierarchy. *Phys. Rev. B* **78**, 195125 (2008).
- [4] Moore, G. & Read, N. Nonabelions in the fractional quantum Hall effect. *Nucl. Phys. B* **360**, 362-396 (1991).
- [5] Read, N. & Green, D. Paired states of fermions in two dimensions with breaking of parity and time-reversal symmetries and the fractional quantum Hall effect. *Phys. Rev. B* **61**, 10267-10297 (2000).
- [6] Kitaev, A. Y. Unpaired Majorana fermions in quantum wires. *Phys.-Usp.* **44**, 131-136 (2001).
- [7] Kitaev, A. Fault-tolerant quantum computation by anyons. *Ann. Phys.* **303**, 2-30 (2003).
- [8] Das Sarma, S., Freedman, M. & Nayak, C. Topologically protected qubits from a possible non-Abelian fractional quantum Hall state. *Phys. Rev. Lett.* **94**, 166802 (2005).
- [9] Nayak, C., Simon, S. H., Stern, A., Freedman, M. & Das Sarma, S. Non-Abelian anyons and topological quantum computation. *Rev. Mod. Phys.* **80**, 1083-1159 (2008).
- [10] Fu, L. & Kane, C. L. Superconducting proximity effect and Majorana fermions at the surface of a topological insulator. *Phys. Rev. Lett.* **100**, 096407 (2008).
- [11] Sau, J. D., Lutchyn, R. M., Tewari, S. & Das Sarma, S. Generic new platform for topological quantum computation using semiconductor heterostructures. *Phys. Rev. Lett.* **104**, 040502 (2010).
- [12] Alicea, J. Majorana fermions in a tunable semiconductor device. *Phys. Rev. B* **81**, 125318 (2010).
- [13] Lutchyn, R. M., Sau, J. D. & Das Sarma, S. Majorana fermions and a topological phase transition in semiconductor-superconductor heterostructures. *Phys. Rev. Lett.* **105**, 077001 (2010).
- [14] Oreg, Y., Refael, G. & von Oppen, F. Helical liquids and Majorana bound states in quantum wires. *Phys. Rev. Lett.* **105**, 177002 (2010).
- [15] Potter, A. C. & Lee, P. A. Multichannel generalization of Kitaev's Majorana end states and a practical route to realize them in thin films. *Phys. Rev. Lett.* **105**, 227003 (2010).
- [16] Law, K. T., Lee, P. A. & Ng, T. K. Majorana fermion induced resonant Andreev reflection. *Phys. Rev. Lett.* **103**, 237001 (2009).
- [17] Mourik, V. *et al.* Signatures of Majorana Fermions in Hybrid Superconductor-Semiconductor Nanowire Devices. *Science* **336**, 1003-1007 (2012).
- [18] Deng, M. T. *et al.* Observation of Majorana fermions in a Nb-InSb nanowire-Nb hybrid quantum device. *Nano Lett.* **12**, 6414-6419 (2012).
- [19] Das, A. *et al.* Zero-bias peaks and splitting in an Al-InAs nanowire topological superconductor as a signature of Majorana fermions. *Nature Phys.* **8**, 887-895 (2012).
- [20] Qi, X. -L., Hughes, T. L., Raghu, S. & Zhang, S. -C. Time-Reversal-Invariant topological superconductors and superfluids in two and three dimensions. *Phys. Rev. Lett.* **102**, 187001 (2009).
- [21] Teo, J. C. Y., & Kane, C. L. Topological Defects and Gapless Modes in Insulators and Superconductors. *Phys. Rev. B* **82**, 115120 (2010).
- [22] Schnyder, A. P., Brydon, P. M. R., Manske D. & Timm, C. Andreev spectroscopy and surface density of states for a three-dimensional time-reversal invariant topological superconductor. *Phys. Rev. B* **82**, 184508 (2010).
- [23] Beenakker, C. W. J., Dahlhaus, J. P., Wimmer, M. & Akhmerov A. R. Random-matrix theory of Andreev reflection from a topological superconductor, *Phys. Rev. B* **83**, 085413 (2011).
- [24] Deng, S., Viola, L., & Ortiz, G. Majorana modes in time-reversal invariant s-wave topological superconductors. *Phys. Rev. Lett.* **108**, 036803 (2012).
- [25] Nakosai, S., Tanaka, Y. & Nagaosa, N. Topological superconductivity in bilayer Rashba system. *Phys. Rev. Lett.* **108**, 147003 (2012).
- [26] Wong, L. M. & Law, K. T. Realizing DIII class topological superconductors using $d_{x^2-y^2}$ -wave superconductors. *Phys. Rev. B* **86**, 184516 (2012).
- [27] Zhang, F., Kane, C. L. & Mele, E. J. Time Reversal Invariant Topological Superconductivity and Majorana Kramers Pairs. Preprint at <http://arxiv.org/abs/1212.4232> (2012).
- [28] Nakosai, S., Budich, J. C., Tanaka, Y., Trauzettel, B., & Nagaosa, N. Majorana bound states and non-local spin correlations in a quantum wire on an unconventional superconductor. *Phys. Rev. Lett.* **110**, 117002 (2013).
- [29] Bauer, E. *et al.* Heavy Fermion Superconductivity and Magnetic Order in Noncentrosymmetric CePt₃Si. *Phys. Rev. Lett.* **92**, 027003 (2004).
- [30] Liu, X. -J. & Lobos, A. M. Manipulating Majorana fermions in quantum nanowires with broken inversion symmetry. *Phys. Rev. B* **87**, 060504(R) (2013).

Supplementary Information

In this Supplementary Material we provide the details of the results presented in the main text. In particular, we study in detail the proximity effect of a non-centrosymmetric superconductor in a conducting nanowire, the fermion parity conservation for each sector of the time-reversal partners, the braiding statistics of Majorana end modes in DIII class 1D topological superconductor, and the Josephson effect for the measurement of topological qubit states in a DIII class superconductor.

S-1. TOPOLOGICAL SUPERCONDUCTOR OF DIII CLASS BY PROXIMITY EFFECT

The DIII class 1D topological superconductor can be engineered by depositing a conducting quantum wire on a non-centrosymmetric superconductor thin-film which induces s - and p -wave pairings in the wire by proximity effect. The total Hamiltonian of the heterostructure system reads $H = H_{\text{SC}} + H_{\text{wire}} + H_{\text{t}}$, where H_{SC} , H_{wire} , and H_{t} represent the Hamiltonian for the substrate superconductor, the conducting wire, and the tunneling at the interface, respectively.

Due to the presence of spin-orbit coupling, a typical non-centrosymmetric superconductor has both p -wave and s -wave pairings. To differentiate from the notations used for the nanowire, we denote by the pairings in the superconductor by $\Delta_s^{(0)}$ and $\Delta_p^{(0)}$, respectively. The BdG Hamiltonian for the 2D non-centrosymmetric superconductor is given by

$$H_{SC} = \sum_{k_x, k_y} [\xi(k_x, k_y)\tau_z + \alpha_R^{(0)} \sin k_y \sigma_x - \alpha_R^{(0)} \sin k_x \sigma_y \tau_z + \Delta_p^{(0)} \sin k_y \sigma_z \tau_x - \Delta_p^{(0)} \sin k_x \tau_y - \Delta_s^{(0)} \sigma_y \tau_y], \quad (S1)$$

where $\xi(k_x, k_y) = -2t^{(0)}(\cos k_x + \cos k_y) - \mu^{(0)}$ is the normal dispersion relation with $t^{(0)}$ the hopping coefficient in the superconductor, σ_j and τ_j ($j = x, y, z$) are the Pauli matrices acting on the spin and Nambu spaces, respectively, $\alpha_R^{(0)}$ is the spin-orbit coupling coefficient, and $\mu^{(0)}$ is chemical potential. The pairing order parameters can be reorganized by $\hat{\Delta} = (\Delta_s^{(0)} + \mathbf{d} \cdot \boldsymbol{\sigma})(i\sigma_y)$, with the \mathbf{d} -vectors defined as $\mathbf{d} = \Delta_p^{(0)}(-\sin k_y, \sin k_x, 0)$. In the above Hamiltonian we take that the \mathbf{g} -vector for spin-orbit coupling, given by $\mathbf{g} = \alpha_R^{(0)}(\sin k_y, -\sin k_x)$, is antiparallel to \mathbf{d} .

A single-channel 1D conducting quantum wire, being put along the x axis, can be described by the following Hamiltonian

$$H_{\text{wire}} = \sum_{k_x} (-2t_w \cos k_x - \mu_w) \tau_z, \quad (S2)$$

with t_w the hopping coefficient and μ_w the chemical potential in the wire. It is noteworthy that the intrinsic spin-orbit interaction is not needed to reach the TRI topological superconducting phase in the nanowire, while the proximity effect can induce an effective spin-orbit interaction in the wire. Finally, we give the tunneling Hamiltonian H_t for the interface. Assuming that at the interface the coupling between the substrate superconductor and the nanowire is uniform along the wire, the momentum k_x is still a good quantum number (we note that this assumption can be relaxed for the existence of Majorana fermions in the topological phase). Then the tunneling Hamiltonian can be written down as

$$H_t = -t_{\perp} \sum_{k_x, \sigma} c_{i_y, \sigma}^{\dagger}(k_x) d_{i_y, \sigma}(k_x) + h.c., \quad (S3)$$

where $\sigma = \uparrow, \downarrow$ are the spin indices, t_{\perp} denotes the tunneling coefficient between the nanowire and substrate superconductor, $c_{i_y, \sigma}^{\dagger}, c_{i_y, \sigma}$ and $d_{i_y, \sigma}^{\dagger}, d_{i_y, \sigma}$ are the creation and annihilation operators of electrons for the quantum wire and the superconductor, respectively. The site number i_y characterizes where the heterostructure locates along y axis in the non-centrosymmetric superconductor.

The induced superconductivity in the wire can be obtained by integrating out the degree of freedom of the superconductor substrate, and will be calculated numerically, as described below. We perform the integration in two steps. First, consider that the non-centrosymmetric superconductor is uniform, and we determine the Green's function $G_s(k_x, i_y)$ of the substrate superconductor with momentum k_x and at the site i_y below the nanowire by standard recursive method [1]. Then, the coupling of the nanowire to the superconductor can be reduced to the coupling to the site i_y below the wire and described by the Green's function $G_s(k_x, i_y)$. Integrating out the degree of freedom of the sites in the superconductor right below the nanowire yields a self-energy for the Green's function of the nanowire, which gives rise to the proximity effect. The effective Green's function of the nanowire takes the form

$$G_{\text{wire}}^{\text{eff}}(i\omega, k_x) = \frac{1}{i\omega - \xi(k_x)\tau_z - \Sigma(i\omega)}, \quad (S4)$$

where the self-energy reads $\Sigma(i\omega) = t_{\perp}^2 G_s(k_x, i_y)$. Finally the spectral function is determined by

$$A(\omega, k_x) = -\frac{1}{2\pi} \Im \{ \text{Tr} [\tau_z G_{\text{wire}}^{\text{eff}}(\omega + i0^+, k_x)] \}, \quad (S5)$$

with \Im taking the imaginary part, Tr denoting the trace over the spin and Nambu spaces, and 0^+ a positive infinitesimal. The spectral function determines the bulk band structure, which is numerically shown in Fig. S1 with different chemical potentials of the nanowire. In particular, from the numerical results we find that the nanowire is in the topologically nontrivial regime when $|\mu_w| < 2|t_w|$ and $|\Delta_p^{(0)}| > |\Delta_s^{(0)}|$ which leads to the induced pairings in the wire $|\Delta_p| > |\Delta_s|$, while it is in the trivial regime when $|\Delta_s^{(0)}| > |\Delta_p^{(0)}|$ or $|\mu_w| > 2|t_w|$ (i.e. the chemical potential is tuned out of the band of the wire). When tuning the chemical potential down to the band bottom, the bulk gap in the nanowire is reduced and closes right at the bottom, implying the critical value of the chemical potential $\mu_w^c = -2t_w$ (similar results can be obtained around $2t_w$, the top of the band) [Fig. S1 (a-b)]. In the topological regime at each

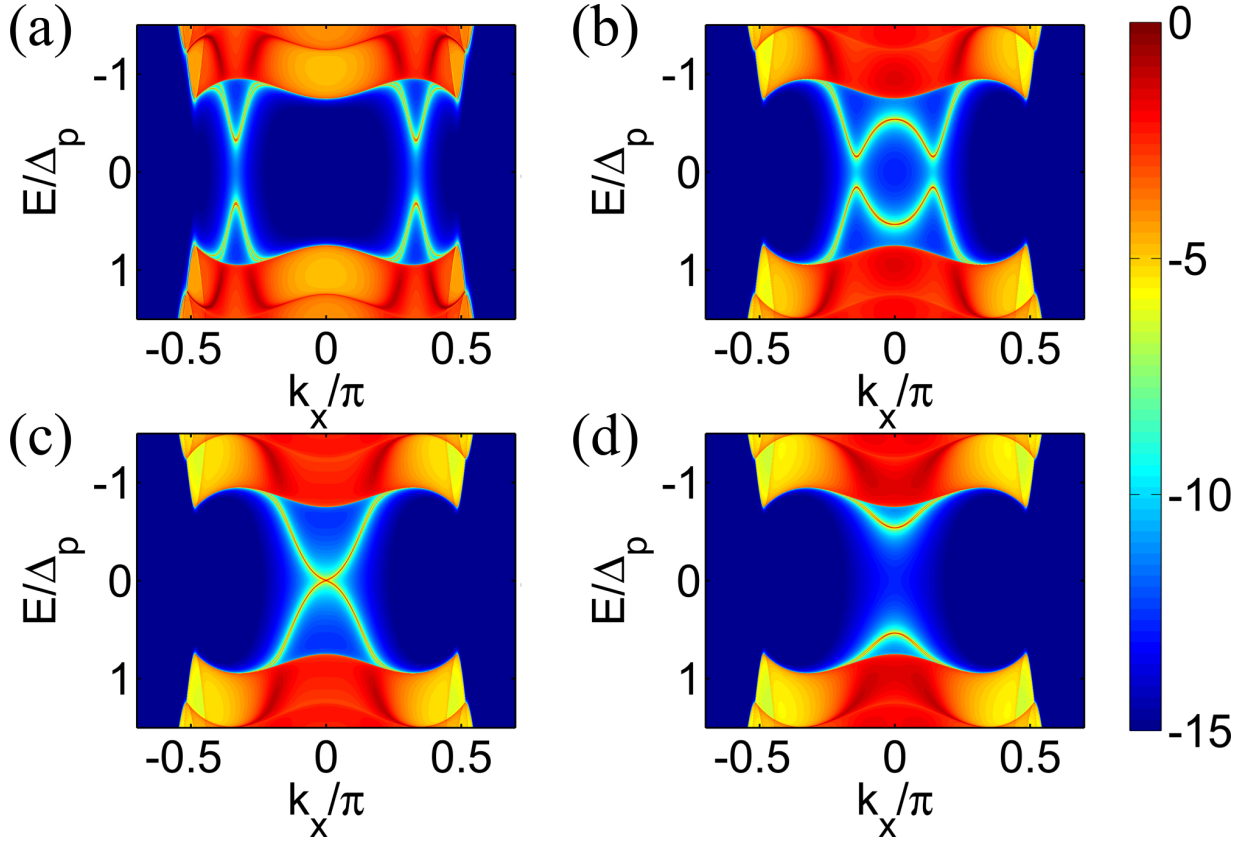


FIG. S1: The logarithmic plot of the spectral function for the nanowire/non-centrosymmetric superconductor heterostructure. The yellow dotted curves show the bulk band structure of the nanowire system. The red solid areas (in the upper and lower positions of each panel) represent the bulk states of the substrate superconductor. (a) Topological regime with the chemical potential μ_w set as $-2t_w + 5|\Delta_p^{(0)}|$ in the nanowire. In this regime at each end of the wire localized two Majorana zero modes [Fig. S2]. (b) Topological regime with reduced bulk gap by tuning $\mu_w = -2t_w + |\Delta_p^{(0)}|$ close to the band bottom. (c) Critical point $\mu_w^c = -2t_w$ for the topological phase transition with the bulk gap closed. (d) Trivial phase regime for the nanowire with $\mu_w = -2t_w - |\Delta_p^{(0)}|$. Other parameters are taken that $t_\perp = 0.5t_w = 0.5t^{(0)}$, $|\Delta_s| = 0.5|\Delta_p|$, and $\alpha_R^{(0)} = |\Delta_p|$.

end of the nanowire are localized two Majorana zero modes γ_j and $\tilde{\gamma}_j$ ($j = L, R$), with their wave functions shown in Fig. S2. Further lowering the chemical potential reopens the bulk gap, and the system is driven into a trivial phase [Fig. S1 (d)].

It is interesting that the phase diagram in the nanowire does not depend on the parameter details of the couplings between the wire and the substrate superconductor, and the topological regime in the wire can be obtained in a large parameter range that $-2t_w < \mu_w < 2t_w$ when $|\Delta_p^{(0)}| > |\Delta_s|^{(0)}$. With such a large window for the topological phase, the present proposal shows advantages in engineering the DIII class topological states of the wire by simply tuning μ_w to be below or above the band bottom of the wire.

S-2. FERMION PARITY CONSERVATION

Fermion parity measures the even and odd numbers of the fermions in a quantum system. For a superconductor because of the pairing gap the number of fermions can only vary by pairs, which leads to the fermion parity conservation. Therefore, the total fermion parity is always conserved in a DIII class 1D topological superconductor. Moreover, in this section we show in detail that in a DIII class 1D topological SC the fermion parity is actually conserved for each sector of the time-reversal partners, more than for the total system. It is trivial to know that this result is true if the DIII class topological superconductor is composed of two decoupled copies (for instance, corresponding to spin-up and spin-down, respectively) of 1D chiral p -wave superconductors. The each copy of the chiral p -wave superconductor conserves the fermion parity conservation. Therefore, for the proof we shall focus on the generic DIII class topological superconductor where the TRI couplings are allowed between different copies of time-reversal partners.

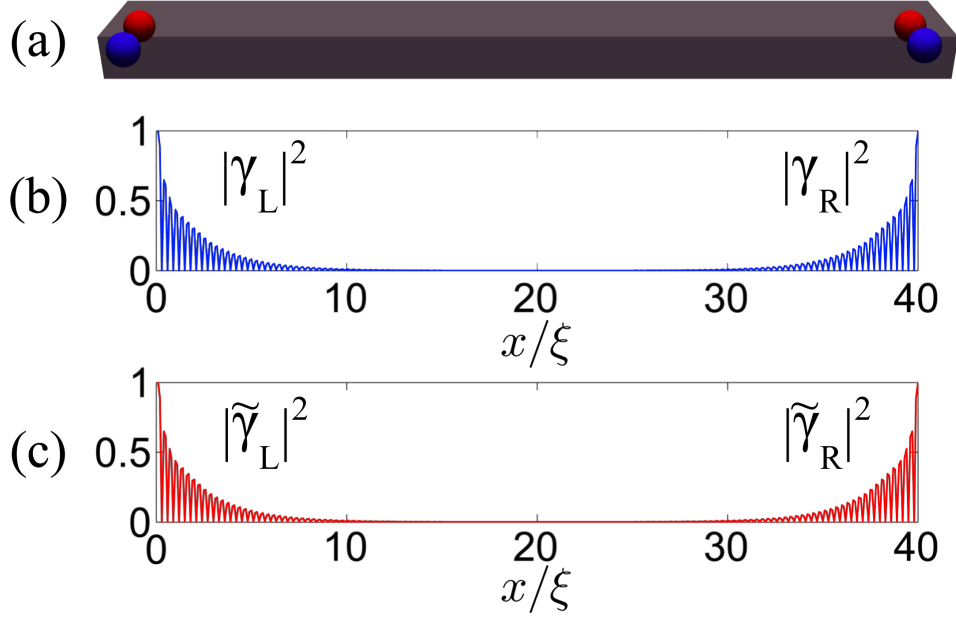


FIG. S2: (a) Two Majorana bound modes exist at each end of the nanowire in the topological regime with $\mu = -2t_w + |\Delta_p^{(0)}|$ as considered in Fig. S1. (b-c) The wave functions of two Majorana modes $\gamma_{L/R}$ and $\tilde{\gamma}_{L/R}$ at the same end have exactly the same spatial profile, with ξ the coherence length in the nanowire.

We consider a single Majorana quantum wire, which hosts four Majorana end modes denoted by $\gamma_{1,2}$ and $\tilde{\gamma}_{1,2}$ and transformed by time-reversal operator that $\mathcal{T}^{-1}\gamma_j\mathcal{T} = \tilde{\gamma}_j$ and $\mathcal{T}^{-1}\tilde{\gamma}_j\mathcal{T} = -\gamma_j$ [2]. With the four Majorana states we can define two non-local complex fermions by $f_1 = \frac{1}{2}(\gamma_1 + i\gamma_2)$, $\tilde{f}_1 = \frac{1}{2}(\tilde{\gamma}_1 - i\tilde{\gamma}_2)$, which germinate four topological qubit states $|n_1\tilde{n}_1\rangle$ with $n_1, \tilde{n}_1 = 0, 1$. The proof of fermion parity conservation for each sector is equivalent to showing that the four topological qubit states $|n_1\tilde{n}_1\rangle$ are generically decoupled from each other with the presence of TRI perturbations in the Majorana modes.

Note that the coupling between the Majorana modes localized at the same end of the nanowire, γ_j and $\tilde{\gamma}_j$, breaks time-reversal symmetry. The coupling Hamiltonian in terms of Majorana end modes should take the following generic TRI form

$$V(\lambda) = iE_1(\lambda)(\gamma_1\gamma_2 - \tilde{\gamma}_1\tilde{\gamma}_2) + iE_2(\lambda)(\gamma_1\tilde{\gamma}_2 - \gamma_2\tilde{\gamma}_1), \quad (\text{S6})$$

where we assume that the couplings $E_{1,2}(\lambda)$ depend on an experimentally manipulatable parameter λ . The above Hamiltonian can be rewritten in the block diagonal form with new Majorana bases that

$$V(\lambda) = iE(\lambda)[\gamma^{(1)}\gamma^{(2)} - \tilde{\gamma}^{(1)}\tilde{\gamma}^{(2)}] \quad (\text{S7})$$

where $\gamma^{(1)} = \gamma_1$, $\tilde{\gamma}^{(1)} = \tilde{\gamma}_1$, $\gamma^{(2)} = \sin\theta\gamma_2 + \cos\theta\tilde{\gamma}_2$, $\tilde{\gamma}^{(2)} = \sin\theta\tilde{\gamma}_2 - \cos\theta\gamma_2$, and $E = \sqrt{E_1^2 + E_2^2}$. The mixing angle θ is defined via $\tan\theta = E_1/E_2$. The complex fermions $f^{(1)}$ and $\tilde{f}^{(1)}$ in the eigen-basis are then defined by

$$f^{(1)} = \frac{1}{2}[\gamma^{(1)} + i\gamma^{(2)}], \quad (\text{S8})$$

$$\tilde{f}^{(1)} = \frac{1}{2}[\tilde{\gamma}^{(1)} - i\tilde{\gamma}^{(2)}]. \quad (\text{S9})$$

It is easy to know that the even parity eigenstates $|0\tilde{0}\rangle$ and $|1\tilde{1}\rangle$ germinated by $f^{(1)}$ and $\tilde{f}^{(1)}$ acquire an energy splitting $2E(\lambda)$, while the odd parity states $|0\tilde{1}\rangle$ and $|1\tilde{0}\rangle$ are still degenerate. To prove the fermion parity conservation for each sector, we need to confirm that all the four topological qubit states $|n_1\tilde{n}_1\rangle$ can evolve adiabatically when the coupling Hamiltonian $V(\lambda)$ changes with the parameter λ . Since $|1\tilde{0}\rangle$ and $|0\tilde{1}\rangle$ form a Kramers' doublet, the transition between them is forbidden by the time-reversal symmetry. Therefore, we only need to consider the adiabatic condition for the two even parity states. The fermion parity conservation for each sector is guaranteed when the following adiabatic condition is satisfied in the manipulation

$$|\langle 11 | \frac{\partial \lambda}{\partial t} \frac{\partial}{\partial \lambda} | 00 \rangle| \ll 2|E(\lambda)|. \quad (\text{S10})$$

It should be noted that the adiabatic condition needs to be justified only in the presence of finite couplings. When $E(\lambda) \rightarrow 0$, the couplings between Majorana end modes vanish and then all the topological qubit states are automatically decoupled from each other. One can verify that

$$\frac{\partial f^{(1)}}{\partial \lambda} = \frac{i}{2} \frac{\partial \theta}{\partial \lambda} (\cos \theta \gamma_2 - \sin \theta \tilde{\gamma}_2) = \frac{1}{2} \frac{\partial \theta}{\partial \lambda} (\tilde{f}^{(1)\dagger} - \tilde{f}^{(1)}), \quad (\text{S11})$$

$$\frac{\partial \tilde{f}^{(1)}}{\partial \lambda} = -\frac{i}{2} \frac{\partial \theta}{\partial \lambda} (\cos \theta \tilde{\gamma}_2 + \sin \theta \gamma_2) = -\frac{1}{2} \frac{\partial \theta}{\partial \lambda} (f^{(1)\dagger} - f^{(1)}). \quad (\text{S12})$$

In the above formulas the derivative of the bases $\gamma_j, \tilde{\gamma}_j$ with respect to λ does not contribute to the left hand side of Eq. (S10), and is neglected. The condition (S10) then reads

$$\left| \frac{\partial \lambda}{\partial t} \frac{\partial \theta}{\partial \lambda} \right| \ll 4|E(\lambda)|. \quad (\text{S13})$$

We show below that the above condition is generically satisfied in the realistic materials.

According to the the previous section, with the proximity induced p -wave and s -wave superconducting pairings, the effective tight-binding Hamiltonian in the nanowire can be written as

$$\begin{aligned} H_{\text{wire}}^{\text{eff}} = & \sum_{\langle i,j \rangle, \sigma} t_{ij} c_{i\sigma}^\dagger c_{j\sigma} + \sum_{\langle i,j \rangle} (t_{ij}^{\text{so}} c_{i\uparrow}^\dagger c_{j\downarrow} + \text{H.c.}) + \sum_{\langle i,j \rangle} (\Delta_{ij}^p c_{i\uparrow} c_{j\uparrow} + \Delta_{ij}^{p*} c_{i\downarrow} c_{j\downarrow} + \text{H.c.}) + \sum_j (\Delta_s c_{j\uparrow} c_{j\downarrow} + \text{H.c.}) \\ & - \mu \sum_{j,\sigma} n_{j\sigma} + \sum_{j,\sigma} V_j^{\text{dis}} n_{j\sigma}, \end{aligned} \quad (\text{S14})$$

where the hopping coefficients and the chemical potential are generically renormalized by the proximity effect. Without loss of generality, in the above Hamiltonian we have taken into account the spin-orbit interaction described by the t_{ij}^{so} term, and the random on-site disorder potential V_j^{dis} with $\langle V_j^{\text{dis}} \rangle = 0$. For the case with uniform pairing orders, the parameters Δ_s and Δ_p can be taken as real. On the other hand, for one-dimensional system, the phases in the (spin-orbit) hopping coefficients can always be absorbed into electron operators. Therefore, in the following study we consider that all the parameters in $H_{\text{wire}}^{\text{eff}}$ are real numbers.

In the topological regime, at each end of the wire we obtain two Majorana zero modes which are transformed to each other by time-reversal operator. In terms of the electron operators, these bound modes take the form

$$\gamma_1 = \sum_j [u_\uparrow^{(1)}(x_j) c_\uparrow(x_j) + u_\downarrow^{(1)}(x_j) c_\downarrow(x_j) + u_\uparrow^{(1)*}(x_j) c_\uparrow^\dagger(x_j) + u_\downarrow^{(1)*}(x_j) c_\downarrow^\dagger(x_j)], \quad (\text{S15})$$

$$\tilde{\gamma}_1 = \sum_j [u_\uparrow^{(1)*}(x_j) c_\downarrow(x_j) - u_\downarrow^{(1)*}(x_j) c_\uparrow(x_j) + u_\uparrow^{(1)}(x_j) c_\downarrow^\dagger(x_j) - u_\downarrow^{(1)}(x_j) c_\uparrow^\dagger(x_j)], \quad (\text{S16})$$

$$\gamma_2 = i \sum_j [u_\uparrow^{(2)}(x_j) c_\uparrow(x_j) + u_\downarrow^{(2)}(x_j) c_\downarrow(x_j) - u_\uparrow^{(2)*}(x_j) c_\uparrow^\dagger(x_j) - u_\downarrow^{(2)*}(x_j) c_\downarrow^\dagger(x_j)], \quad (\text{S17})$$

$$\tilde{\gamma}_2 = i \sum_j [u_\uparrow^{(2)*}(x_j) c_\downarrow(x_j) - u_\downarrow^{(2)*}(x_j) c_\uparrow(x_j) - u_\uparrow^{(2)}(x_j) c_\downarrow^\dagger(x_j) + u_\downarrow^{(2)}(x_j) c_\uparrow^\dagger(x_j)]. \quad (\text{S18})$$

Since the coefficients in $H_{\text{wire}}^{\text{eff}}$ are real, we have that $u_{\uparrow,\downarrow}^{(1,2)} = u_{\uparrow,\downarrow}^{(1,2)*}$. The coupling energies between the Majorana modes at left $(\gamma_1, \tilde{\gamma}_1)$ and right $(\gamma_2, \tilde{\gamma}_2)$ ends are calculated by $E_1 = i\langle \gamma_1 | H_{\text{wire}}^{\text{eff}} | \gamma_2 \rangle = -i\langle \tilde{\gamma}_1 | H_{\text{wire}}^{\text{eff}} | \tilde{\gamma}_2 \rangle$ and $E_2 = i\langle \gamma_1 | H_{\text{wire}}^{\text{eff}} | \tilde{\gamma}_2 \rangle = -i\langle \tilde{\gamma}_1 | H_{\text{wire}}^{\text{eff}} | \gamma_2 \rangle$. Using the relations

$$c_{j\uparrow} \simeq u_\uparrow^{(1)}(x_j) \gamma_1 - u_\downarrow^{(1)}(x_j) \tilde{\gamma}_1 - i u_\uparrow^{(2)}(x_j) \gamma_2 + i u_\downarrow^{(2)}(x_j) \tilde{\gamma}_2, \quad (\text{S19})$$

$$c_{j\downarrow} \simeq u_\downarrow^{(1)}(x_j) \gamma_1 + u_\uparrow^{(1)}(x_j) \tilde{\gamma}_1 - i u_\downarrow^{(2)}(x_j) \gamma_2 - i u_\uparrow^{(2)}(x_j) \tilde{\gamma}_2, \quad (\text{S20})$$

we obtain that

$$E_1 = \sum_{\langle i,j \rangle \sigma} t_{ij} u_\sigma^{(1)}(x_i) u_\sigma^{(2)}(x_j) + \sum_{\langle i,j \rangle \sigma} \Delta_{ij}^p u_\sigma^{(1)}(x_i) u_\sigma^{(2)}(x_j) + \sum_{\langle i,j \rangle} t_{ij}^{\text{so}} [u_\uparrow^{(1)}(x_i) u_\downarrow^{(2)}(x_j) + u_\downarrow^{(1)}(x_j) u_\uparrow^{(2)}(x_i)] \\ + \sum_j \Delta_s [u_\uparrow^{(1)}(x_j) u_\downarrow^{(2)}(x_j) - u_\downarrow^{(1)}(x_j) u_\uparrow^{(2)}(x_j)] + \sum_{j,\sigma} V_j^{\text{dis}} u_\sigma^{(1)}(x_j) u_\sigma^{(2)}(x_j), \quad (\text{S21})$$

$$E_2 = \sum_{\langle i,j \rangle} t_{ij} [u_\uparrow^{(1)}(x_i) u_\downarrow^{(2)}(x_j) - u_\downarrow^{(1)}(x_i) u_\uparrow^{(2)}(x_j)] + \sum_{\langle i,j \rangle} \Delta_{ij}^p [u_\uparrow^{(1)}(x_i) u_\downarrow^{(2)}(x_j) - u_\downarrow^{(1)}(x_i) u_\uparrow^{(2)}(x_j)] \\ + \sum_{\langle i,j \rangle} t_{ij}^{\text{so}} [u_\uparrow^{(1)}(x_i) u_\uparrow^{(2)}(x_j) - u_\downarrow^{(1)}(x_j) u_\downarrow^{(2)}(x_i)] + \sum_j \Delta_s [u_\uparrow^{(1)}(x_j) u_\uparrow^{(2)}(x_j) + u_\downarrow^{(1)}(x_j) u_\downarrow^{(2)}(x_j)] \\ + \sum_{j,\sigma} V_j^{\text{dis}} [u_\uparrow^{(1)}(x_j) u_\downarrow^{(2)}(x_j) - u_\downarrow^{(1)}(x_j) u_\uparrow^{(2)}(x_j)]. \quad (\text{S22})$$

Note that $t_{ij}^{\text{so}} = -t_{ji}^{\text{so}}$ and for a uniform nanowire we expect that $\sum_{\langle i,j \rangle} u_\uparrow^{(1)}(x_i) u_\downarrow^{(2)}(x_j) = \sum_{\langle i,j \rangle} u_\uparrow^{(2)}(x_i) u_\downarrow^{(1)}(x_j)$ and $\sum_j u_\uparrow^{(1)}(x_j) u_\downarrow^{(2)}(x_j) = \sum_j u_\uparrow^{(2)}(x_j) u_\downarrow^{(1)}(x_j)$. With these properties we find that in E_1 the terms corresponding to t_{ij}^{so} and Δ_s vanish, while in E_2 the terms for t_{ij} , Δ_p , and V_j^{dis} vanish. We then have

$$E_1 = \sum_{\langle i,j \rangle \sigma} t_{ij} u_\sigma^{(1)}(x_i) u_\sigma^{(2)}(x_j) + \sum_{\langle i,j \rangle \sigma} \Delta_{ij}^p u_\sigma^{(1)}(x_i) u_\sigma^{(2)}(x_j) + \sum_{j,\sigma} V_j^{\text{dis}} u_\sigma^{(1)}(x_j) u_\sigma^{(2)}(x_j), \quad (\text{S23})$$

$$E_2 = \sum_{\langle i,j \rangle \sigma} t_{ij}^{\text{so}} u_\sigma^{(1)}(x_i) u_\sigma^{(2)}(x_j) + \sum_{j,\sigma} \Delta_s u_\sigma^{(1)}(x_j) u_\sigma^{(2)}(x_j). \quad (\text{S24})$$

The wave functions of Majorana bound modes decay exponentially as a function of the distance from the end of the nanowire, multiplying by an oscillatory function with the oscillating period equal to the Fermi wavelength in the nanowire. This implies that $u_\sigma^{(1)} \propto \sin(k_F x) e^{-x/\xi}$ and $u_\sigma^{(2)} \propto \sin[k_F(L-x)] e^{-(L-x)/\xi}$, where ξ is the effective coherence length of the wire. In the realistic material, we consider that the chemical potential in the nanowire is far below the half-filling condition and thus $k_F a \ll 1$. In this way we have $u_\sigma^{(1)}(x_j) u_\sigma^{(2)}(x_j) \approx u_\sigma^{(1)}(x_j) u_\sigma^{(2)}(x_{j\pm 1}) e^{\mp a/\xi}$. Furthermore, the coherence length is typically much larger than the lattice constant $\xi \gg a$, and we can further approximate that $u_\sigma^{(1)}(x_j) u_\sigma^{(2)}(x_j) \approx u_\sigma^{(1)}(x_j) u_\sigma^{(2)}(x_{j\pm 1})$. Bearing this result in mind we get

$$E_1 = \sum_{\langle i,j \rangle \sigma} t_{ij} u_\sigma^{(1)}(x_i) u_\sigma^{(2)}(x_j) + \sum_{\langle i,j \rangle \sigma} \Delta_{ij}^p u_\sigma^{(1)}(x_i) u_\sigma^{(2)}(x_j) + \sum_{j,\sigma} V_j^{\text{dis}} u_\sigma^{(1)}(x_j) u_\sigma^{(2)}(x_j), \quad (\text{S25})$$

$$E_2 = \sum_{\langle i,j \rangle \sigma} t_{ij}^{\text{so}} u_\sigma^{(1)}(x_i) u_\sigma^{(2)}(x_j) + \sum_{\langle i,j \rangle \sigma} \Delta_s u_\sigma^{(1)}(x_i) u_\sigma^{(2)}(x_j). \quad (\text{S26})$$

The spin-orbit hopping coefficient $t_{ij}^{\text{so}} = -t_{ji}^{\text{so}}$ and the p -wave pairing $\Delta_{ij}^p = -\Delta_{ji}^p$ are staggered parameters. In the limit that $k_F a \ll 1$ and $\xi \gg a$, the summation for such two terms in E_1 and E_2 also turns out to be zero. On the other hand, the spin-conserved hopping is a constant and we denote $t_{ij} = t_{ji} = t$. Finally, if the the random potential V_j^{dis} with $\langle V_j^{\text{dis}} \rangle = 0$ is distributed homogeneously in the nanowire, we expect that the last term in E_1 gives $V_0 \sum_{j,\sigma} u_\sigma^{(1)}(x_j) u_\sigma^{(2)}(x_j)$ with the constant factor V_0 depending on the specific disorder profile and much less than the amplitude of the disorder potential. The couplings $E_{1,2}$ become

$$E_1 \simeq (t + V_0) \sum_{\langle i,j \rangle \sigma} u_\sigma^{(1)}(x_i) u_\sigma^{(2)}(x_j), \quad (\text{S27})$$

$$E_2 \simeq \Delta_s \sum_{\langle i,j \rangle \sigma} u_\sigma^{(1)}(x_i) u_\sigma^{(2)}(x_j). \quad (\text{S28})$$

From the above result we find that $E_2/E_1 \approx \Delta_s/(t + V_0)$, which is consistent with the fact that when $\Delta_s = 0$ the original Hamiltonian (S14) can be block diagonalized and then $E_2 = 0$. This implies that in the realistic nanowire materials while the magnitudes of $E_{1,2}(\lambda)$ depend on λ which determines the overlapping between the wave functions of Majorana bound modes at left and right ends, their ratio is nearly a constant. Therefore we always have

$$\frac{\partial \theta}{\partial \lambda} \approx 0, \quad (\text{S29})$$

which validates the adiabatic condition. The results in the Eqs. (S27) and (S28) have a simple physical picture. Being proportional to the overlapping between the wave functions of Majorana bound modes at different ends, the couplings $E_{1,2}$ are exponential decaying functions of the nanowire length. Since the Majorana modes γ_j and $\tilde{\gamma}_j$ are connected by \mathcal{T} -transformation, their wave functions have exactly the same spatial profile, which leads to the same exponential form for the couplings $E_{1,2}(\lambda) = \alpha_{1,2}(\lambda)e^{-d/\xi}$ with d the distance between the left and right Majorana end modes. The pre-factors $\alpha_j(\lambda)$ depend on the local couplings, including the hopping coefficients, pairings, and so on, between electrons belonging to the same (for $j = 1$) or different (for $j = 2$) sectors of the time-reversal partners. For the case with constant and homogeneous local couplings, we have that their ratio α_1/α_2 is proportional to the ratio of couplings between electrons of the same and different sectors, and is nearly a constant, justifying the adiabatic condition. The above derivative is clearly confirmed with numerical results in the realistic systems with the presence of random on-site disorder scattering, as shown in Fig. S3.

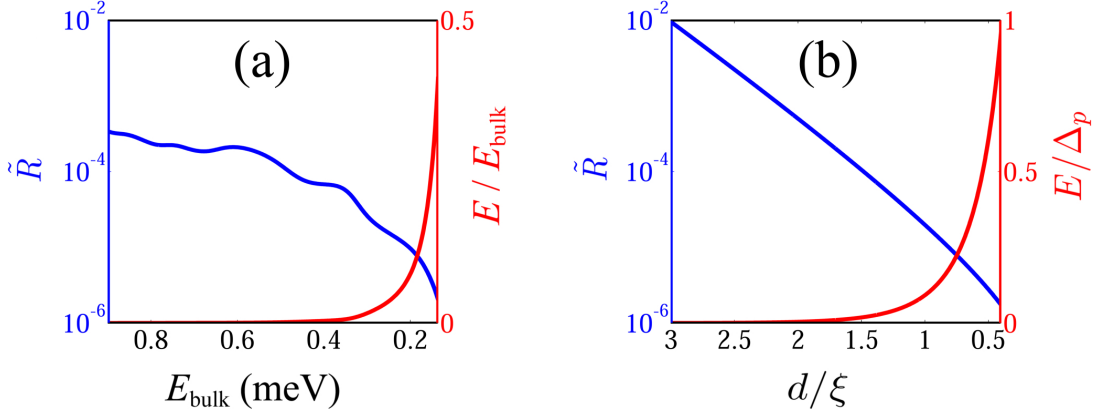


FIG. S3: Adiabatic condition and fermion parity conservation for each sector of time-reversal partners in the presence of disorder scattering. The energy splitting E between $|0\tilde{0}\rangle$ and $|1\tilde{1}\rangle$ (red curves) and the ratio \tilde{R} (blue curves) versus (a) the bulk gap which varies by tuning the chemical potential, and (b) the distance between the Majorana end modes. In the numerical simulation the random on-site disorder potential is considered, with the potential amplitude $V_{\text{dis}} \sim 1.0$ meV. Other parameters in the nanowire are taken that $\Delta_p = 1.0$ meV, $\Delta_s = 0.5$ meV, and $E_{\text{so}} = 0.1$ meV. The coupling energy E is tuned from 0 to 1.0 meV within the time $1.0\mu\text{s}$.

It is noteworthy that for fixed parameter λ , the physics of the fermion parity conservation for each sector can also be easily understood. For DIII class topological superconductor, the helical p -wave pairings occur between two electrons belonging to the same sector of the time-reversal partners. While the change by one in the fermion number of each sector conserves the total fermion parity of the system, it changes fermion parity for each sector, and thus breaks a p -wave Cooper pair in each sector. This process costs finite energy and is thus suppressed by the p -wave pairing gap if Δ_p dominates over Δ_s and the time-reversal symmetry is not broken. The previous study in this section further proves this conservation law when the coupling Hamiltonian between Majorana end modes is adjusted adiabatically.

The fermion parity conservation for each sector has several important physical implications. First, this conservation law shows that an isolated DIII class 1D Majorana wire should stay in one of the four fermion parity eigenstates germinated by non-local complex fermion operators $f_j^{(1)}$ and $\tilde{f}_j^{(1)}$, as long as time-reversal symmetry is not broken. In particular, one can always prepare a nanowire initially in the ground qubit state $|0\tilde{0}\rangle$ or $|1\tilde{1}\rangle$ by controlling the couplings (e.g. through tuning the bulk gap) between Majorana modes at different ends of the wire, and then manipulate the states adiabatically. Furthermore, for a single wire, the two topological qubit states with the same total fermion parity, e.g. $|0\tilde{0}\rangle$ and $|1\tilde{1}\rangle$ are physically different states. In the last section of this Supplementary Material, we shall show that these states can be distinguished in the experiment. This is explicitly different from the situation in a chiral topological superconductor, where two states with the same total fermion parity are not distinguishable. To simplify the notations in the further discussion, we relabel the block diagonal Majorana modes $\gamma_j^{(1)}, \tilde{\gamma}_j^{(1)}$ as $\gamma_j, \tilde{\gamma}_j$. Accordingly, the diagonal complex fermion modes are redefined as f_j, \tilde{f}_j .

S-3. BRAIDING STATISTICS

With the fermion parity conservation for each sector we shall show below that the exchange of Majorana zero modes in DIII class superconductor is generically equivalent to two independent processes of braiding Majorana fermions of

two different sectors, respectively. The physics can be understood in the following way. First of all, since the bulk is gapped, braiding adiabatically the Majorana zero modes, e.g. $\gamma_1, \tilde{\gamma}_1$ and $\gamma_2, \tilde{\gamma}_2$, does not affect the bulk states. Furthermore, assuming that other Majorana zero modes are located far away from the two exchanged pairs, in the braiding we only need to consider the evolution of the Majorana zero modes which are braided. Finally, since the fermion parity is conserved for each sector, in the braiding the two complex fermion modes f_1 and \tilde{f}_1 are always decoupled and their dynamics can be derived independently. In this section we study in detail the braiding matrix for the DIII class 1D topological superconductor.

A. Degenerate ground state

We first construct the generic degenerate ground states for the DIII class 1D topological superconductor. Consider that the 1D Majorana wire has $2M$ pairs of Majorana zero modes $\gamma_1, \tilde{\gamma}_1; \gamma_2, \tilde{\gamma}_2; \dots$, and $\gamma_{2M}, \tilde{\gamma}_{2M}$, with different pairs of Majorana zero modes well separated from each other. With these modes we can define the M pairs of complex fermion modes by $f_j = (\gamma_{2j-1} + i\gamma_{2j})/2$ and $\tilde{f}_j = (\tilde{\gamma}_{2j-1} - i\tilde{\gamma}_{2j})/2$, with $j = 1, \dots, M$. It follows that

$$\mathcal{T}^{-1}f_j\mathcal{T} = \tilde{f}_j, \quad \mathcal{T}^{-1}\tilde{f}_j\mathcal{T} = -f_j. \quad (\text{S30})$$

For the bulk states, we denote the Bogoliubov-de Gennes quasiparticle operators with positive energies by d_η and \tilde{d}_η , with $\tilde{d}_\eta = \mathcal{T}^{-1}d_\eta\mathcal{T}$. Let $|\text{vac}\rangle$ be the vacuum state with respect to the electron operators and we construct the wave function

$$|\psi\rangle = \frac{1}{\sqrt{\mathcal{N}}} \prod_{\alpha} d_{\alpha} \prod_{\beta} \tilde{d}_{\beta} |\text{vac}\rangle. \quad (\text{S31})$$

Here $\sqrt{\mathcal{N}}$ is the normalization factor. It is clear that $|\psi\rangle$ is an eigenstate of $f_j^\dagger f_j$ and $\tilde{f}_j^\dagger \tilde{f}_j$ with eigenvalue n_j and \tilde{n}_j , respectively. Note that n_j and \tilde{n}_j can be either 1 or 0, and their magnitudes depend on the convention used in defining the Majorana wave functions [3, 4]. To be concrete, we shall use the convention that

$$|\psi\rangle = |11\dots 1\rangle |\tilde{1}\tilde{1}\dots \tilde{1}\rangle. \quad (\text{S32})$$

The ground state with $n_j = \tilde{n}_j = 0$ is then constructed by

$$|00\dots 0\rangle |\tilde{0}\tilde{0}\dots \tilde{0}\rangle = f_1 \dots f_M \tilde{f}_1 \dots \tilde{f}_1 |\psi\rangle, \quad (\text{S33})$$

and generically

$$|n_1 \dots n_M\rangle |\tilde{n}_1 \dots \tilde{n}_M\rangle = \prod_j^M f_j^{1-n_j} \prod_j^M \tilde{f}_j^{1-\tilde{n}_j} |\psi\rangle. \quad (\text{S34})$$

B. General results for the braiding process

Now we study the general results of the braiding process. In particular, we shall show that braiding two pairs of Majorana zero modes $\gamma_j, \tilde{\gamma}_j$ and $\gamma_{j+1}, \tilde{\gamma}_{j+1}$ can be reduced to two independent processes of exchanging γ_j, γ_{j+1} and $\tilde{\gamma}_j, \tilde{\gamma}_{j+1}$, respectively. During the braiding process, the Hamiltonian $H(\lambda)$ generically depends on an adiabatic parameter λ , and at any fixed λ -value the time-reversal symmetry is preserved. There are two different contributions which may affect the exchange dynamics. One is the Berry phase effect in the degenerate ground subspace, and another is that after the exchange, the original ground state subspace may vary and evolve into new forms. This study is similar as that in the chiral topological superconductors [3, 4], but with the new ingredients of time-reversal symmetry and fermion parity conservation for each sector of the time-reversal partners.

B.1. Berry phase effect

In the braiding, the Hamiltonian and the many-body ground state vary with the adiabatic parameter λ . To determine the Berry phase in the braiding, we calculate the Berry's connection by

$$A_{n,m}(\lambda) = i\hbar \langle n_1 \dots n_M | \langle \tilde{n}_1 \dots \tilde{n}_M | \partial_\lambda | m_1 \dots m_M \rangle | \tilde{m}_1 \dots \tilde{m}_M \rangle. \quad (\text{S35})$$

Since we only braid the two pairs of Majorana zero modes $\gamma_1, \tilde{\gamma}_1$ and $\gamma_2, \tilde{\gamma}_2$, we can assume that only these four Majorana zero modes are λ -dependent, while all other Majorana modes are independent of λ [4]. Then, from Eq. (S34) we know that

$$A_{n,m}(\lambda) = A_{n_1 \tilde{n}_1, m_1 \tilde{m}_1} \delta_{n_2 m_2} \delta_{\tilde{n}_2 \tilde{m}_2} \dots \delta_{n_M m_M} \delta_{\tilde{n}_M \tilde{m}_M}, \quad (\text{S36})$$

where

$$\begin{aligned} A_{n_1 \tilde{n}_1, m_1 \tilde{m}_1}(\lambda) &= i\hbar \langle n_1; \tilde{n}_1 | \partial_\lambda | m_1; \tilde{m}_1 \rangle \\ &= A_{n_1 \tilde{n}_1, m_1 \tilde{m}_1}^{(1)}(\lambda) + A_{n_1 \tilde{n}_1, m_1 \tilde{m}_1}^{(2)}(\lambda) + A_{n_1 \tilde{n}_1, m_1 \tilde{m}_1}^{(3)}(\lambda). \end{aligned} \quad (\text{S37})$$

For the last line of the above formula we have that

$$\begin{aligned} A_{n_1 \tilde{n}_1, m_1 \tilde{m}_1}^{(1)}(\lambda) &= i\hbar \langle \psi(\lambda) | [\tilde{f}_1^\dagger]^{1-\tilde{n}_1} [f_1^\dagger]^{1-n_1} [f_1]^{1-m_1} [\tilde{f}_1]^{1-\tilde{m}_1} \partial_\lambda | \psi(\lambda) \rangle, \\ A_{n_1 \tilde{n}_1, m_1 \tilde{m}_1}^{(2)}(\lambda) &= i\hbar (1-m_1) \langle \psi(\lambda) | [\tilde{f}_1^\dagger]^{1-\tilde{n}_1} [f_1^\dagger]^{1-n_1} (\partial_\lambda f_1) [\tilde{f}_1]^{1-\tilde{m}_1} | \psi(\lambda) \rangle, \\ A_{n_1 \tilde{n}_1, m_1 \tilde{m}_1}^{(3)}(\lambda) &= i\hbar (1-\tilde{m}_1) \langle \psi(\lambda) | [\tilde{f}_1^\dagger]^{1-\tilde{n}_1} [f_1^\dagger]^{1-n_1} [f_1]^{1-m_1} (\partial_\lambda \tilde{f}_1) | \psi(\lambda) \rangle. \end{aligned} \quad (\text{S38})$$

From the former section we have shown that the Fermi parity is conserved for each sector of the time-reversal partners, and therefore we have $A_{n_1 \tilde{n}_1, m_1 \tilde{m}_1} = 0$ for $n_1 \neq m_1$ or $\tilde{n}_1 \neq \tilde{m}_1$. On the other hand, the continuous variation of λ cannot change the fermion numbers which are discrete values, which implies that

$$\partial_\lambda |\psi(\lambda)\rangle \propto |\psi(\lambda)\rangle, \quad (\text{S39})$$

and therefore we have

$$A_{n_1 \tilde{n}_1, m_1 \tilde{m}_1}^{(j)}(\lambda) = A_{n_1 \tilde{n}_1}^{(j)}(\lambda) \delta_{n_1 m_1} \delta_{\tilde{n}_1 \tilde{m}_1}, \quad j = 1, 2, 3. \quad (\text{S40})$$

It is easy to check that $A_{n_1 \tilde{n}_1}^{(1)}(\lambda)$ is independent of n_1 and \tilde{n}_1 . To calculate $A_{n_1 \tilde{n}_1, m_1 \tilde{m}_1}^{(2)}(\lambda)$ and $A_{n_1 \tilde{n}_1, m_1 \tilde{m}_1}^{(3)}(\lambda)$, we need to examine $\partial_\lambda f_1$ and $\partial_\lambda \tilde{f}_1$, which can be generally decomposed as

$$\begin{aligned} \partial_\lambda f_1(\lambda) &= u(\lambda) f_1(\lambda) + u'(\lambda) f_1^\dagger(\lambda) + v(\lambda) \tilde{f}_1(\lambda) + v'(\lambda) \tilde{f}_1^\dagger(\lambda) + \sum_\alpha [a(\lambda) d_\alpha(\lambda) + a'(\lambda) d_\alpha^\dagger(\lambda)] \\ &\quad + \sum_\alpha [b(\lambda) \tilde{d}_\alpha(\lambda) + b'(\lambda) \tilde{d}_\alpha^\dagger(\lambda)] \end{aligned} \quad (\text{S41})$$

$$\begin{aligned} \partial_\lambda \tilde{f}_1(\lambda) &= \tilde{u}(\lambda) \tilde{f}_1(\lambda) + \tilde{u}'(\lambda) \tilde{f}_1^\dagger(\lambda) + \tilde{v}(\lambda) f_1(\lambda) + \tilde{v}'(\lambda) f_1^\dagger(\lambda) + \sum_\alpha [\tilde{a}(\lambda) \tilde{d}_\alpha(\lambda) + \tilde{a}'(\lambda) \tilde{d}_\alpha^\dagger(\lambda)] \\ &\quad + \sum_\alpha [\tilde{b}(\lambda) d_\alpha(\lambda) + \tilde{b}'(\lambda) d_\alpha^\dagger(\lambda)]. \end{aligned} \quad (\text{S42})$$

Fermion modes composed of other Majorana zero states are neglected in the above expansion since they are far away from f_1 and \tilde{f}_1 . Note that the terms corresponding to bulk quasi-particle operators d_α and \tilde{d}_α cannot contribute to the Berry's connection. Therefore for simplicity we also neglect them in the further discussion. From the time-reversal transformation of the two complex fermion operators $\mathcal{T}^{-1} f_1 \mathcal{T} = \tilde{f}_1$, $\mathcal{T}^{-1} \tilde{f}_1 \mathcal{T} = -f_1$, we have the following restrictions in the coefficients

$$u(\lambda) = u^*(\lambda), \quad u'(\lambda) = [u'(\lambda)]^*, \quad v(\lambda) = -\tilde{v}^*(\lambda), \quad v'(\lambda) = -[v'(\lambda)]^*. \quad (\text{S43})$$

The fermion parity conservation for each sector requires that $v(\lambda) = v'(\lambda) = 0$. Therefore we have

$$\begin{aligned} \partial_\lambda f_1(\lambda) &= u(\lambda) f_1(\lambda) + u'(\lambda) f_1^\dagger(\lambda), \\ \partial_\lambda \tilde{f}_1(\lambda) &= u^*(\lambda) \tilde{f}_1(\lambda) + u'^*(\lambda) \tilde{f}_1^\dagger(\lambda). \end{aligned}$$

Substituting the above formulas into the second and third lines in Eqs. (S38) we get then

$$\begin{aligned} A_{n_1 \tilde{n}_1, m_1 \tilde{m}_1}^{(2)}(\lambda) &= i\hbar (1-m_1) u(\lambda) \delta_{n_1 m_1} \delta_{\tilde{n}_1 \tilde{m}_1}, \\ A_{n_1 \tilde{n}_1, m_1 \tilde{m}_1}^{(3)}(\lambda) &= i\hbar (1-\tilde{m}_1) u^*(\lambda) \delta_{n_1 m_1} \delta_{\tilde{n}_1 \tilde{m}_1}. \end{aligned} \quad (\text{S44})$$

Furthermore, it can be shown that

$$\begin{aligned} u(\lambda) \propto \langle \psi(\lambda) | f_1^\dagger (\partial_\lambda f_1) | \psi(\lambda) \rangle &= \frac{i}{2} \langle \psi(\lambda) | \partial_\lambda (\gamma_1 \gamma_2) | \psi(\lambda) \rangle \\ &= 0, \end{aligned} \quad (\text{S45})$$

where we have used the results that $\gamma_j^2(\lambda) = 1$ and the overlapping between γ_1 and γ_2 is negligible. With these results in mind we have $A_{n_1 \tilde{n}_1, m_1 \tilde{m}_1}^{(2,3)}(\lambda) = 0$, and conclude that

$$\begin{aligned} A_{n_1 \tilde{n}_1, m_1 \tilde{m}_1}(\lambda) &= A(\lambda) \delta_{n_1 m_1} \delta_{\tilde{n}_1 \tilde{m}_1} \delta_{n_2 m_2} \delta_{\tilde{n}_2 \tilde{m}_2} \dots \delta_{n_M m_M} \delta_{\tilde{n}_M \tilde{m}_M} \\ &= i\hbar \langle \psi(\lambda) | \partial_\lambda | \psi(\lambda) \rangle \delta_{n_1 m_1} \delta_{\tilde{n}_1 \tilde{m}_1} \delta_{n_2 m_2} \delta_{\tilde{n}_2 \tilde{m}_2} \dots \delta_{n_M m_M} \delta_{\tilde{n}_M \tilde{m}_M}, \end{aligned} \quad (\text{S46})$$

which is independent of n_j and \tilde{n}_j . Since the Berry's connection is diagonal and identical for all qubit states, the Berry phase effect does not bring any nontrivial contribution to the braiding process. This effect is similar as the situation in the chiral topological superconductors.

B.2. Ground state variation

The nontrivial effect for the exchange of two pairs of Majorana zero modes can be resulted from the fact that each ground state itself $|n_1 \dots n_M\rangle |\tilde{n}_1 \dots \tilde{n}_M\rangle$ can change after the braiding process. Actually, the final state is generically related to the initial one via (after braiding $\gamma_1, \tilde{\gamma}_1$ and $\gamma_2, \tilde{\gamma}_2$)

$$|n_1 \dots n_M\rangle |\tilde{n}_1 \dots \tilde{n}_M\rangle_{\text{final}} = e^{i\theta(n_1, \tilde{n}_1)} |n_1 n_2 \dots n_M\rangle |\tilde{n}_1 \tilde{n}_2 \dots \tilde{n}_M\rangle_{\text{initial}}. \quad (\text{S47})$$

We can always choose $\theta(1, 1) = 0$. Since the off-diagonal Berry's connection is zero, the above results show that braiding Majorana zero modes $\gamma_1, \tilde{\gamma}_1$ and $\gamma_2, \tilde{\gamma}_2$ is equivalent to two independent processes of exchanging γ_1 and γ_2 , and $\tilde{\gamma}_1$ and $\tilde{\gamma}_2$, respectively. For the complex fermion operators, we have $f_1(\lambda_{\text{final}}) = e^{i\theta(1,0)} f_1(\lambda_{\text{initial}})$ and $\tilde{f}_1(\lambda_{\text{final}}) = e^{i\theta(0,1)} \tilde{f}_1(\lambda_{\text{initial}})$. From the time-reversal symmetry we have that $\theta(1, 0) = -\theta(0, 1)$. This leads to

$$\begin{aligned} |1n_2 \dots n_M\rangle |\tilde{1}\tilde{n}_2 \dots \tilde{n}_M\rangle_{\text{final}} &= |1n_2 \dots n_M\rangle |1\tilde{n}_2 \dots \tilde{n}_M\rangle_{\text{initial}}, \\ |1n_2 \dots n_M\rangle |\tilde{0}\tilde{n}_2 \dots \tilde{n}_M\rangle_{\text{final}} &= e^{i\theta_0} |1n_2 \dots n_M\rangle |0\tilde{n}_2 \dots \tilde{n}_M\rangle_{\text{initial}}, \\ |0n_2 \dots n_M\rangle |\tilde{1}\tilde{n}_2 \dots \tilde{n}_M\rangle_{\text{final}} &= e^{-i\theta_0} |0n_2 \dots n_M\rangle |1\tilde{n}_2 \dots \tilde{n}_M\rangle_{\text{initial}}, \\ |0n_2 \dots n_M\rangle |\tilde{0}\tilde{n}_2 \dots \tilde{n}_M\rangle_{\text{final}} &= |0n_2 \dots n_M\rangle |0\tilde{n}_2 \dots \tilde{n}_M\rangle_{\text{initial}}, \end{aligned}$$

where $\theta_0 \equiv \theta(1, 0) = -\theta(0, 1)$. In the next subsection we shall prove that $\theta_0 = \pi/2$. Then the braiding matrix is given by $U_{12} = e^{\frac{\pi}{4}\gamma_1\gamma_2} e^{\frac{\pi}{4}\tilde{\gamma}_1\tilde{\gamma}_2}$, which explicitly respects the time-reversal symmetry.

C. Braiding phases

Since the exchange dynamics is proved to be equivalent to two independent processes of braiding the Majorana zero modes $\gamma_1, \tilde{\gamma}_1$ and $\gamma_2, \tilde{\gamma}_2$, respectively, we can construct a toy model of the DIII class Majorana quantum wire to study the braiding phases. The simplest case is a two-copy of 1D Kitaev model [5] with spin-1/2 fermions respecting the time-reversal symmetry. A T-junction is needed and can be formed by a vertical wire (along y axis) which has N sites, and a horizontal wire (along x direction) which has $2N + 1$ sites. The N th site of the vertical wire connects to the $N + 1$ th site of the vertical wire. Moreover, we consider that in the topological region of the T-junction, the hopping term equals to the pairing term $t = \Delta$. We model the Hamiltonian that

$$\begin{aligned} H &= -\mu \sum_{\sigma; y=1}^N c_{y,\sigma}^\dagger c_{y,\sigma} + |t| \sum_{x=1}^{2N+1} [(e^\phi c_{x,\uparrow}^\dagger + e^{-\phi} c_{x,\uparrow})(e^\phi c_{x+1,\uparrow}^\dagger - e^{-\phi} c_{x+1,\uparrow}) \\ &\quad + (e^{-\phi} c_{x,\downarrow}^\dagger + e^\phi c_{x,\downarrow})(e^{-\phi} c_{x+1,\downarrow}^\dagger - e^\phi c_{x+1,\downarrow})], \end{aligned} \quad (\text{S48})$$

where ϕ is the hopping and pairing phase for the vertical wire and $\mu < 0$ is the chemical potential for the horizontal wire. The chemical potential for the horizontal wire, the hopping and pairing in the vertical wire are set to be zero. In this configuration the vertical wire of the T-junction is initially in the trivial phase and the horizontal wire in the

topological phase. Note the braiding dynamics should be independent of ϕ , we shall consider $\phi = 0$ for simplicity, and then

$$H = -\mu \sum_{\sigma; y=1}^N c_{y,\sigma}^\dagger c_{y,\sigma} + t \sum_{x=1}^{2N} [(c_{x,\uparrow}^\dagger - c_{x,\uparrow})(c_{x+1,\uparrow}^\dagger + c_{x+1,\uparrow}) + (c_{x,\downarrow}^\dagger - c_{x,\downarrow})(c_{x+1,\downarrow}^\dagger + c_{x+1,\downarrow})]. \quad (\text{S49})$$

With the above model, we have four decoupled Majorana zero bound states, $\gamma_{1,\uparrow,\downarrow}$ and $\gamma_{2N+1,\uparrow,\downarrow}$, localized at two end sites. The initial four degenerate ground states are given by

$$\begin{aligned} |1\rangle|\tilde{1}\rangle_{\text{initial}} &= \frac{1}{2^{2N}} \prod_{\sigma=\uparrow,\downarrow} \left[1 + \sum_{p=0}^N \sum_{i_1 < \dots < i_{2p}}^{2N+1} c_{i_{2p},\sigma}^\dagger \dots c_{i_1,\sigma}^\dagger \right] |\text{vac}\rangle, \\ |1\rangle|\tilde{0}\rangle_{\text{initial}} &= \frac{1}{2^{2N}} \left[1 + \sum_{p=0}^N \sum_{i_1 < \dots < i_{2p}}^{2N+1} c_{i_{2p},\uparrow}^\dagger \dots c_{i_1,\uparrow}^\dagger \right] \left[\sum_{p=0}^N \sum_{i_1 < \dots < i_{2p+1}}^{2N+1} c_{i_{2p+1},\downarrow}^\dagger \dots c_{i_1,\downarrow}^\dagger \right] |\text{vac}\rangle, \\ |0\rangle|\tilde{1}\rangle_{\text{initial}} &= \frac{1}{2^{2N}} \left[\sum_{p=0}^N \sum_{i_1 < \dots < i_{2p+1}}^{2N+1} c_{i_{2p+1},\uparrow}^\dagger \dots c_{i_1,\uparrow}^\dagger \right] \left[1 + \sum_{p=0}^N \sum_{i_1 < \dots < i_{2p}}^{2N+1} c_{i_{2p},\downarrow}^\dagger \dots c_{i_1,\downarrow}^\dagger \right] |\text{vac}\rangle, \\ |0\rangle|\tilde{0}\rangle_{\text{initial}} &= \frac{1}{2^{2N}} \prod_{\sigma=\uparrow,\downarrow} \sum_{p=0}^N \sum_{i_1 < \dots < i_{2p+1},\sigma}^{2N+1} c_{i_{2p+1},\sigma}^\dagger \dots c_{i_1,\sigma}^\dagger |\text{vac}\rangle. \end{aligned}$$

It is straightforward to verify that for all above states the average number of electrons is $\bar{N} = 2N + 1$.

The Majorana end modes can be transported by tuning adiabatically the parameters μ and $t (= \Delta)$ in the T-junction [4]. After the braiding the Majorana modes $\gamma_{1,\uparrow,\downarrow}$ and $\gamma_{2N+1,\uparrow,\downarrow}$ exchange their positions, which can be pictorially described by reversing the hopping and pairing direction in the Hamiltonian (S49). This implies that after braiding the new Hamiltonian is obtained by taking $t \rightarrow -t$, since the hopping and pairing to the left and right directions in Eq. (S49) explicitly have opposite sign. Therefore we get the new Hamiltonian

$$H' = -\mu \sum_{\sigma; y=1}^N c_{y,\sigma}^\dagger c_{y,\sigma} - t \sum_{x=1}^{2N} [(c_{x,\uparrow}^\dagger - c_{x,\uparrow})(c_{x+1,\uparrow}^\dagger + c_{x+1,\uparrow}) + (c_{x,\downarrow}^\dagger - c_{x,\downarrow})(c_{x+1,\downarrow}^\dagger + c_{x+1,\downarrow})]. \quad (\text{S50})$$

The corresponding new ground states then read

$$\begin{aligned} |1\rangle|\tilde{1}\rangle_m &= \frac{1}{2^{2N}} \prod_{\sigma=\uparrow,\downarrow} \left[1 + \sum_{p=0}^N \sum_{i_1 < \dots < i_{2p}}^{2N+1} (-1)^p c_{i_{2p},\sigma}^\dagger \dots c_{i_1,\sigma}^\dagger \right] |\text{vac}\rangle, \\ |1\rangle|\tilde{0}\rangle_m &= \frac{1}{2^{2N}} \left[1 + \sum_{p=0}^N \sum_{i_1 < \dots < i_{2p}}^{2N+1} (-1)^p c_{i_{2p},\uparrow}^\dagger \dots c_{i_1,\uparrow}^\dagger \right] \left[\sum_{p=0}^N \sum_{i_1 < \dots < i_{2p+1}}^{2N+1} (-1)^p c_{i_{2p+1},\downarrow}^\dagger \dots c_{i_1,\downarrow}^\dagger \right] |\text{vac}\rangle, \\ |0\rangle|\tilde{1}\rangle_m &= \frac{1}{2^{2N}} \left[\sum_{p=0}^N \sum_{i_1 < \dots < i_{2p+1}}^{2N+1} (-1)^p c_{i_{2p+1},\uparrow}^\dagger \dots c_{i_1,\uparrow}^\dagger \right] \left[1 + \sum_{p=0}^N \sum_{i_1 < \dots < i_{2p}}^{2N+1} (-1)^p c_{i_{2p},\downarrow}^\dagger \dots c_{i_1,\downarrow}^\dagger \right] |\text{vac}\rangle, \\ |0\rangle|\tilde{0}\rangle_m &= \frac{1}{2^{2N}} \prod_{\sigma=\uparrow,\downarrow} \sum_{p=0}^N \sum_{i_1 < \dots < i_{2p+1},\sigma}^{2N+1} (-1)^p c_{i_{2p+1},\sigma}^\dagger \dots c_{i_1,\sigma}^\dagger |\text{vac}\rangle. \end{aligned}$$

To finish the braiding, we need to adiabatically transform H' back to the initial form H . This can be performed by considering the following Hamiltonian

$$\begin{aligned} H_\lambda &= -\mu \sum_{\sigma; y=1}^N c_{y,\sigma}^\dagger c_{y,\sigma} - t \sum_{x=1}^{2N} \left[(e^{-i\lambda\pi/2} c_{x,\uparrow}^\dagger - e^{i\lambda\pi/2} c_{x,\uparrow})(e^{-i\lambda\pi/2} c_{x+1,\uparrow}^\dagger + e^{i\lambda\pi/2} c_{x+1,\uparrow}) + \right. \\ &\quad \left. + (e^{i\lambda\pi/2} c_{x,\downarrow}^\dagger - e^{-i\lambda\pi/2} c_{x,\downarrow})(e^{i\lambda\pi/2} c_{x+1,\downarrow}^\dagger + e^{-i\lambda\pi/2} c_{x+1,\downarrow}) \right], \end{aligned} \quad (\text{S51})$$

where λ is an adiabatic parameter. The adiabatic ground states are given by

$$\begin{aligned}
|1\rangle|\tilde{1}\rangle_\lambda &= \frac{1}{2^{2N}} \prod_{\sigma=\uparrow,\downarrow} \left[1 + \sum_{p=0}^N \sum_{i_1 < \dots < i_{2p}}^{2N+1} (-1)^p e^{-i\sigma_z \lambda \pi p} c_{i_{2p},\sigma}^\dagger \dots c_{i_1,\sigma}^\dagger \right] |\text{vac}\rangle, \\
|1\rangle|\tilde{0}\rangle_\lambda &= \frac{1}{2^{2N}} \left[1 + \sum_{p=0}^N \sum_{i_1 < \dots < i_{2p}}^{2N+1} (-1)^p e^{-i\lambda \pi p} c_{i_{2p},\uparrow}^\dagger \dots c_{i_1,\uparrow}^\dagger \right] \left[\sum_{p=0}^N \sum_{i_1 < \dots < i_{2p+1}}^{2N+1} (-1)^p e^{i\lambda \pi (p+1/2)} c_{i_{2p+1},\downarrow}^\dagger \dots c_{i_1,\downarrow}^\dagger \right] |\text{vac}\rangle, \\
|0\rangle|\tilde{1}\rangle_\lambda &= \frac{1}{2^{2N}} \left[\sum_{p=0}^N \sum_{i_1 < \dots < i_{2p+1}}^{2N+1} (-1)^p e^{-i\lambda \pi (p+1/2)} c_{i_{2p+1},\uparrow}^\dagger \dots c_{i_1,\uparrow}^\dagger \right] \left[1 + \sum_{p=0}^N \sum_{i_1 < \dots < i_{2p}}^{2N+1} (-1)^p e^{i\lambda \pi p} c_{i_{2p},\downarrow}^\dagger \dots c_{i_1,\downarrow}^\dagger \right] |\text{vac}\rangle, \\
|0\rangle|\tilde{0}\rangle_\lambda &= \frac{1}{2^{2N}} \prod_{\sigma=\uparrow,\downarrow} \sum_{p=0}^N \sum_{i_1 < \dots < i_{2p+1},\sigma}^{2N+1} (-1)^p e^{-i\sigma_z \lambda \pi (p+1/2)} c_{i_{2p+1},\sigma}^\dagger \dots c_{i_1,\sigma}^\dagger |\text{vac}\rangle,
\end{aligned}$$

From the former subsection we know already that the Berry's phase θ_b is the same for all states. With the above states we can check directly that $\theta_b = 0$ for all states. The vanishing Berry's phase is because the time-reversal partners in each ground state contributes oppositely to the Berry's phase. This is reasonable, since a nonzero diagonal Berry's phase actually breaks time-reversal symmetry. For $\lambda = 0$ we have $H(\lambda) = H'$ and for $\lambda = 1$ the Hamiltonian transforms back to the initial one $H(\lambda = 1) = H$. Therefore at $\lambda = 1$ we obtain the final ground states by

$$|1\rangle|\tilde{1}\rangle_{\text{final}} = |1\rangle|1\rangle_{\text{initial}}, \quad (\text{S52})$$

$$|1\rangle|\tilde{0}\rangle_{\text{final}} = i|1\rangle|\tilde{0}\rangle_{\text{initial}}, \quad (\text{S53})$$

$$|0\rangle|\tilde{1}\rangle_{\text{final}} = -i|0\rangle|\tilde{1}\rangle_{\text{initial}}, \quad (\text{S54})$$

$$|0\rangle|\tilde{0}\rangle_{\text{final}} = |0\rangle|\tilde{0}\rangle_{\text{initial}}. \quad (\text{S55})$$

We therefore complete the proof that the braiding phase $\theta_0 \equiv \theta(1, 0) = -\theta(0, 1) = \pi/2$.

D. Braiding matrix and applications

According to the results in Eqs. (S52) to (S55), the braiding matrix for exchanging $\gamma_j, \tilde{\gamma}_j$ and $\gamma_{j+1}, \tilde{\gamma}_{j+1}$ can be constructed by $U_{j,j+1}(T, \tilde{T}) = e^{\frac{\pi}{4} \gamma_j \gamma_{j+1}} e^{\frac{\pi}{4} \tilde{\gamma}_j \tilde{\gamma}_{j+1}}$, which explicitly respects the time-reversal symmetry. To visualize the non-Abelian statistics, we consider now two DIII Majorana chains, with the two pairs of Majorana zero modes $\gamma_1, \tilde{\gamma}_1$ and $\gamma_2, \tilde{\gamma}_2$ localized in the first chain, and the other two pairs $\gamma_3, \tilde{\gamma}_3$ and $\gamma_4, \tilde{\gamma}_4$ in the second chain. The four complex fermion modes are defined by

$$f_1 = \frac{1}{2}(\gamma_1 + i\gamma_2), f_2 = \frac{1}{2}(\gamma_3 + i\gamma_4), \tilde{f}_1 = \frac{1}{2}(\tilde{\gamma}_1 - i\tilde{\gamma}_2), \tilde{f}_2 = \frac{1}{2}(\tilde{\gamma}_3 - i\tilde{\gamma}_4). \quad (\text{S56})$$

They satisfy the relation $\mathcal{T}^{-1} f_{1,2} \mathcal{T} = \tilde{f}_{1,2}$ and $\mathcal{T}^{-1} \tilde{f}_{1,2} \mathcal{T} = -f_{1,2}$. In terms of the complex fermion modes, the transformation matrix for braiding $\gamma_2, \tilde{\gamma}_2$ and $\gamma_3, \tilde{\gamma}_3$ takes the form

$$U_{23}(T, \tilde{T}) = \frac{1}{2} (1 + i f_2^\dagger f_1^\dagger - i f_2^\dagger \tilde{f}_1 + i f_2 f_1^\dagger - i f_2 \tilde{f}_1) (1 - i \tilde{f}_2^\dagger \tilde{f}_1^\dagger + i \tilde{f}_2^\dagger \tilde{f}_1 - i \tilde{f}_2 \tilde{f}_1^\dagger + i \tilde{f}_2 \tilde{f}_1). \quad (\text{S57})$$

The Hilbert space of the four complex fermions is spanned by sixteen topological qubit states $|n_1 n_2\rangle |\tilde{n}_1 \tilde{n}_2\rangle = (f_1^\dagger)^{n_1} (f_2^\dagger)^{n_2} (\tilde{f}_1^\dagger)^{\tilde{n}_1} (\tilde{f}_2^\dagger)^{\tilde{n}_2} |00\rangle |\tilde{0}\tilde{0}\rangle$, where $n_j, \tilde{n}_j = 0, 1$. The bases can be explicitly written down in the form $(|00\rangle, f_1^\dagger |00\rangle, f_2^\dagger |00\rangle, f_1^\dagger f_2^\dagger |00\rangle) \otimes (|\tilde{0}\tilde{0}\rangle, \tilde{f}_1^\dagger |\tilde{0}\tilde{0}\rangle, \tilde{f}_2^\dagger |\tilde{0}\tilde{0}\rangle, \tilde{f}_1^\dagger \tilde{f}_2^\dagger |\tilde{0}\tilde{0}\rangle)$. With this basis we have further

$$U_{23}(T, \tilde{T}) = \frac{1}{2} \begin{bmatrix} 1 & 0 & 0 & -i \\ 0 & 1 & -i & 0 \\ 0 & -i & 1 & 0 \\ -i & 0 & 0 & 1 \end{bmatrix} \otimes \begin{bmatrix} 1 & 0 & 0 & i \\ 0 & 1 & i & 0 \\ 0 & i & 1 & 0 \\ i & 0 & 0 & 1 \end{bmatrix}. \quad (\text{S58})$$

Using the above braiding matrix and for an arbitrary initial state we can obtain the final state straightforwardly. If the initial state is $|00\rangle|\tilde{0}\tilde{0}\rangle$, for instance, we get

$$\begin{aligned}
U_{23}(T, \tilde{T})|00\rangle|\tilde{0}\tilde{0}\rangle &= \frac{1}{2} (|00\rangle|\tilde{0}\tilde{0}\rangle + |11\rangle|\tilde{1}\tilde{1}\rangle + i|00\rangle|\tilde{1}\tilde{1}\rangle - i|11\rangle|\tilde{0}\tilde{0}\rangle) \\
&= \frac{1}{2} (|0\tilde{0}\rangle_L |0\tilde{0}\rangle_R + |1\tilde{1}\rangle_L |1\tilde{1}\rangle_R + i|1\tilde{0}\rangle_L |1\tilde{0}\rangle_R - i|0\tilde{1}\rangle_L |0\tilde{1}\rangle_R),
\end{aligned} \quad (\text{S59})$$

where the indices L and R represents the left and right Majorana chains, respectively. It is interesting that the above state is generically a four-particle entangled state, which carries rich quantum information depending on different measurement strategies (see the discussion on measurement in the next section). First, for each Majorana wire if we do not distinguish the states of the same total parity (e.g. $|\tilde{1}\tilde{0}\rangle_L$ and $|0\tilde{1}\rangle_L$) in the measurement, in the right hand side of the above state the former two terms are equivalent, and can be denoted as $|L_{\text{even}}\rangle|R_{\text{even}}\rangle$, which implies that both Majorana wires are in the even parity state. Similarly, the later two terms are also equivalent, and can be denoted by $|L_{\text{odd}}\rangle|R_{\text{odd}}\rangle$, implying that both Majorana wires are in the odd parity state. With these notations one can reduce the original state into an effective two-qubit entangled one

$$U_{23}(T, \tilde{T})|00\rangle|\tilde{0}\tilde{0}\rangle = \frac{1}{\sqrt{2}}(|L_{\text{even}}\rangle|R_{\text{even}}\rangle + |L_{\text{odd}}\rangle|R_{\text{odd}}\rangle), \quad (\text{S60})$$

On the other hand, to identify the state (S57) as a four-particle entangled one, we should be able to measure the fermion parity for each sector of the time-reversal partners in a single wire. A novel scheme for the measurement will be proposed and studied in the next section. Similarly, with three Majorana wires of DIII class, we can generate a six-qubit code entanglement through two braiding processes. This shows the natural advantage in generating multi-particle entangled state using DIII class topological superconductors, which can be very useful in the quantum information processing. For example, a five-qubit code entanglement is the minimum requirement to realize an error correcting code [6, 7].

Furthermore, a full braiding, i.e. braiding twice $\gamma_2, \tilde{\gamma}_2$ and $\gamma_3, \tilde{\gamma}_3$ yields the final state by

$$U_{23}^2(T, \tilde{T})|00\rangle|\tilde{0}\tilde{0}\rangle = |1\tilde{1}\rangle|1\tilde{1}\rangle, \quad (\text{S61})$$

which distinguishes from the initial state in that each copy of the p -wave superconductor changes fermion parity. In contrast, a full braiding of two pairs of Majorana fermions in a chiral topological superconductor transforms the state back to the initial one, which is therefore always trivial. From these discussions we find that in the braiding the Majorana modes γ_j do not feel their time-reversal partners $\tilde{\gamma}_j$, which is an essential difference from the situation in exchanging two pairs of Majorana fermions in a chiral superconductor, and makes the braiding operator in a TRI topological superconductor nontrivial.

S-4. JOSEPHSON EFFECT IN THE DIII CLASS 1D TOPOLOGICAL SUPERCONDUCTOR

Now we study how to measure the topological qubit states with the Josephson effect. It has been predicted that in the chiral 1D topological superconductor the Josephson current has 4π periodicity [5], and the topological qubit states for a single wire, $|0\rangle$ and $|1\rangle$, can be detected by measuring the direction of the Josephson currents in the junction [4, 8]. In this section we predict a novel important effect in the Josephson junction formed by DIII class 1D topological superconductor, which provides a feasible scheme to detect the topological qubit states in a TRI Majorana quantum wire.

A. Effective coupling Hamiltonian

We consider a Josephson junction formed by two Majorana nanowire ends with a phase difference $\phi = \phi_R - \phi_L$, as illustrated in Fig. 3(a), and derive the effective coupling Hamiltonian for the Majorana end modes localized at the left (L) and right (R) ends. The electron tunneling process in the junction is described by

$$H_T = \Upsilon c_{L,N}^\dagger c_{R,1} + \Upsilon \tilde{c}_{L,N}^\dagger \tilde{c}_{R,1} + \text{H.c.}, \quad (\text{S62})$$

where $c_{L,N}, \tilde{c}_{L,N}$ and $c_{R,1}, \tilde{c}_{R,1}$ represents the electron operators for the N th site at left and 1st site at right wires of the junction, respectively, and Υ is the tunneling coefficient across the junction. The Majorana end modes can be generically expanded in terms of electron operators

$$\gamma_L = \sum_j (u_{L,j} c_{L,j} + u_{L,j}^* c_{L,j}^\dagger), \quad \tilde{\gamma}_L = \sum_j (\tilde{u}_{L,j} \tilde{c}_{L,j} + \tilde{u}_{L,j}^* \tilde{c}_{L,j}^\dagger), \quad (\text{S63})$$

$$\gamma_R = \sum_j (u_{R,j} c_{R,j} + u_{R,j}^* c_{R,j}^\dagger), \quad \tilde{\gamma}_R = \sum_j (\tilde{u}_{R,j} \tilde{c}_{R,j} + \tilde{u}_{R,j}^* \tilde{c}_{R,j}^\dagger), \quad (\text{S64})$$

where $u_{L/R,j} = \tilde{u}_{L/R,j}^*$ if $\phi_{L/R} = 0$. Note that c_j and \tilde{c}_j represent electron operators of a general time-reversal pair at j th site, not necessarily corresponding to spin-up and spin-down, since the spin is not a good quantum number

when spin-orbit coupling and s -wave order are present (refer to the discussion in Section II). From the above formulas we can solve the electron operators in terms of Majorana and nonzero energy Bogoliubov quasiparticle operators. Reexpressing the Bogoliubov quasiparticles in terms of electron operators we can interpret $c_{L,N}$, $\tilde{c}_{L,N}$ and $c_{R,1}$, $\tilde{c}_{R,1}$ by

$$c_{L,N} = u_{L,N}^* \gamma_L - \sum_{j=1}^N a_{L,j} c_{L,j} - \sum_{j=1}^N b_{L,j}^* c_{L,j}^\dagger, \quad (\text{S65})$$

$$\tilde{c}_{L,N} = \tilde{u}_{L,N}^* \gamma_L - \sum_{j=1}^N \tilde{a}_{L,j} \tilde{c}_{L,j} - \sum_{j=1}^N \tilde{b}_{L,j}^* \tilde{c}_{L,j}^\dagger, \quad (\text{S66})$$

$$c_{R,1} = u_{R,1}^* \gamma_R - \sum_{j=1}^N a_{R,j} c_{R,j} - \sum_{j=1}^N b_{R,j}^* c_{R,j}^\dagger, \quad (\text{S67})$$

$$\tilde{c}_{R,1} = \tilde{u}_{R,1}^* \gamma_R - \sum_{j=1}^N \tilde{a}_{R,j} \tilde{c}_{R,j} - \sum_{j=1}^N \tilde{b}_{R,j}^* \tilde{c}_{R,j}^\dagger, \quad (\text{S68})$$

with a constant normalization factor neglected. Here $a_{L/R,j}$, $\tilde{a}_{L/R,j}$ and $b_{L/R,j}$, $\tilde{b}_{L/R,j}$ are expansion coefficients, originated from the quasiparticle operators other than the corresponding Majorana mode. Substituting these results into the tunneling Hamiltonian H_T yields that

$$\begin{aligned} H_T &= \Upsilon \left(u_{L,N} \gamma_L - \sum_{j=1}^N a_{L,j}^* c_{L,j}^\dagger - \sum_{j=1}^N b_{L,j} c_{L,j} \right) \left(u_{R,1}^* \gamma_R - \sum_{j=1}^N a_{R,j} c_{R,j} - \sum_{j=1}^N b_{R,j}^* c_{R,j}^\dagger \right) + \\ &\quad + \Upsilon \left(\tilde{u}_{L,N} \tilde{\gamma}_L - \sum_{j=1}^N \tilde{a}_{L,j}^* \tilde{c}_{L,j}^\dagger - \sum_{j=1}^N \tilde{b}_{L,j} \tilde{c}_{L,j} \right) \left(\tilde{u}_{R,1}^* \tilde{\gamma}_R - \sum_{j=1}^N \tilde{a}_{R,j} \tilde{c}_{R,j} - \sum_{j=1}^N \tilde{b}_{R,j}^* \tilde{c}_{R,j}^\dagger \right) + \text{H.c.} \\ &\approx \left[\Upsilon u_{L,N} u_{R,1}^* (\phi) \gamma_L \gamma_R + \Upsilon \tilde{u}_{L,N} \tilde{u}_{R,1}^* \tilde{\gamma}_L \tilde{\gamma}_R + \text{H.c.} \right] \\ &\quad - \left[\Upsilon u_{L,N} \gamma_L \left(\sum_{j=1}^N a_{R,j} c_{R,j} + \sum_{j=1}^N b_{R,j}^* c_{R,j}^\dagger \right) + \Upsilon u_{R,1}^* \left(\sum_{j=1}^N a_{L,j}^* c_{L,j}^\dagger + \sum_{j=1}^N b_{L,j} c_{L,j} \right) \gamma_R + \text{H.c.} \right] \\ &\quad - \left[\Upsilon \tilde{u}_{L,N} \tilde{\gamma}_L \left(\sum_{j=1}^N \tilde{a}_{R,j} \tilde{c}_{R,j} + \sum_{j=1}^N \tilde{b}_{R,j}^* \tilde{c}_{R,j}^\dagger \right) + \Upsilon \tilde{u}_{R,1}^* \left(\sum_{j=1}^N \tilde{a}_{L,j}^* \tilde{c}_{L,j}^\dagger + \sum_{j=1}^N \tilde{b}_{L,j} \tilde{c}_{L,j} \right) \tilde{\gamma}_R + \text{H.c.} \right] \\ &= H^{(0)} + H^{(1)}, \end{aligned} \quad (\text{S69})$$

where

$$\begin{aligned} H^{(0)} &= \Upsilon u_{L,N} u_{R,1}^* \gamma_L \gamma_R + \Upsilon \tilde{u}_{L,N} \tilde{u}_{R,1}^* \tilde{\gamma}_L \tilde{\gamma}_R + \text{H.c.}, \\ H^{(1)} &= -\Upsilon u_{L,N} \gamma_L \left(\sum_{j=1}^N a_{R,j} c_{R,j} + \sum_{j=1}^N b_{R,j}^* c_{R,j}^\dagger \right) - \Upsilon u_{R,1}^* \gamma_R \left(\sum_{j=1}^N a_{L,j}^* c_{L,j}^\dagger + \sum_{j=1}^N b_{L,j} c_{L,j} \right) \\ &\quad - \Upsilon \tilde{u}_{L,N} \tilde{\gamma}_L \left(\sum_{j=1}^N \tilde{a}_{R,j} \tilde{c}_{R,j} + \sum_{j=1}^N \tilde{b}_{R,j}^* \tilde{c}_{R,j}^\dagger \right) - \Upsilon \tilde{u}_{R,1}^* \tilde{\gamma}_R \left(\sum_{j=1}^N \tilde{a}_{L,j}^* \tilde{c}_{L,j}^\dagger + \sum_{j=1}^N \tilde{b}_{L,j} \tilde{c}_{L,j} \right) + \text{H.c.} \end{aligned}$$

In the second equation of the formula (S69) we have neglected the higher-order irrelevant terms. The term $H^{(0)}$ represents the direct coupling between Majorana modes at different junction ends, which gives the first term of the effective Hamiltonian H_{eff} in the main text. This can be seen by noticing that

$$\begin{aligned} u_{L,N} &= i|u_{L,N}|e^{i\phi_L/2}, \quad u_{R,1} = |u_{R,1}|e^{i\phi_R/2}, \\ \tilde{u}_{L,N} &= -i|\tilde{u}_{L,N}|e^{i\phi_L/2}, \quad \tilde{u}_{R,1} = |\tilde{u}_{R,1}|e^{i\phi_R/2}, \end{aligned} \quad (\text{S70})$$

with which we can recast $H^{(0)}$ into

$$H^{(0)} = i\Gamma_0 \cos \frac{\phi}{2} (\gamma_L \gamma_R - \tilde{\gamma}_L \tilde{\gamma}_R), \quad \Gamma_0 = 2\Upsilon |u_{L,N} u_{R,1}|. \quad (\text{S71})$$

On the other hand, for $H^{(1)}$ we shall calculate up to the second-order perturbation, which is responsible for the second term of H_{eff} in the main text. From $H^{(1)}$ we know that Majorana modes at one end (e.g. the left end) also couple to the electron modes at another end (the right end). In the second-order perturbation γ_L and $\tilde{\gamma}_L$ (γ_R and $\tilde{\gamma}_R$) couple to c_R and \tilde{c}_R (c_L and \tilde{c}_L), respectively. When a nonzero s -wave pairing is present in the quantum wires, the electrons $c_{L/R}$ and $\tilde{c}_{L/R}$ form a Cooper pair and condense. This process leads to an effective coupling between Majorana zero modes localized at the same end. Therefore, up to the second-order perturbation in the tunneling process, we obtain that

$$H_{\text{eff}}^{(1)} = \frac{1}{2}\Upsilon^2 u_{L,N} \tilde{u}_{L,N} \gamma_L \tilde{\gamma}_L \left[\sum_{j=1}^N a_{R,j} \tilde{a}_{R,j} \int d\tau \langle T_\tau c_{R,j}(\tau) \tilde{c}_{R,j}(0) \rangle + \sum_{j=1}^N b_{R,j}^* \tilde{b}_{R,j}^* \int d\tau \langle T_\tau c_{R,j}^\dagger(\tau) \tilde{c}_{R,j}^\dagger(0) \rangle \right] \\ + \frac{1}{2}\Upsilon^2 u_{R,1} \tilde{u}_{R,1} \gamma_R \tilde{\gamma}_R \left[\sum_{j=1}^N a_{L,j} \tilde{a}_{L,j} \int d\tau \langle T_\tau c_{L,j}(\tau) \tilde{c}_{L,j}(0) \rangle + \sum_{j=1}^N b_{L,j}^* \tilde{b}_{L,j}^* \int d\tau \langle c_{L,j}^\dagger(\tau) \tilde{c}_{L,j}^\dagger(0) \rangle \right] + \text{H.c.} \quad (\text{S72})$$

Here $\int d\tau \langle T_\tau \dots \rangle$ represents time ordered integral. Assuming that the superconducting pairings are uniform in the Majorana nanowires, we obtain from the above formula that

$$H_{\text{eff}}^{(1)} = \frac{1}{2}\Upsilon^2 u_{L,N} \tilde{u}_{L,N} \gamma_L \tilde{\gamma}_L \left[\sum_{j=1}^N a_{R,j} \tilde{a}_{R,j} \sum_k \frac{\Delta_{s,R}^*}{\mathcal{E}_R^2(\Delta_{s,R}; \Delta_{p,R}; k)} - \sum_{j=1}^N b_{R,j}^* \tilde{b}_{R,j}^* \sum_k \frac{\Delta_{s,R}}{\mathcal{E}_R^2(\Delta_{s,R}; \Delta_{p,R}; k)} \right] \\ + \frac{1}{2}\Upsilon^2 u_{R,1} \tilde{u}_{R,1} \gamma_R \tilde{\gamma}_R \left[\sum_{j=1}^N a_{L,j} \tilde{a}_{L,j} \sum_k \frac{\Delta_{s,L}^*}{\mathcal{E}_L^2(\Delta_{s,L}; \Delta_{p,L}; k)} - \sum_{j=1}^N b_{L,j}^* \tilde{b}_{L,j}^* \sum_k \frac{\Delta_{s,L}}{\mathcal{E}_L^2(\Delta_{s,L}; \Delta_{p,L}; k)} \right] + \text{H.c.} \\ = i\Upsilon_L(\phi) \gamma_L \tilde{\gamma}_L + i\tilde{\Upsilon}_R(\phi) \gamma_R \tilde{\gamma}_R, \quad (\text{S73})$$

with $\mathcal{E}_{L/R}(\Delta_{s,R}; \Delta_{p,R}; k)$ the bulk excitation spectra in the left (for L) and right (for R) wires of the junction, respectively. The coupling coefficients read

$$\Upsilon_{L/R}(\phi) = -i\frac{1}{2}\Upsilon^2 u_{L/R,N/1} \tilde{u}_{L/R,N/1} \left[\sum_{j=1}^N a_{R/L,j} \tilde{a}_{R/L,j} \sum_k \frac{\Delta_{s,R/L}^*}{\mathcal{E}_{R/L}^2(\Delta_{s,R/L}; \Delta_{p,R/L}; k)} - \sum_{j=1}^N b_{R/L,j}^* \tilde{b}_{R/L,j}^* \sum_k \frac{\Delta_{s,R/L}}{\mathcal{E}_{R/L}^2(\Delta_{s,R/L}; \Delta_{p,R/L}; k)} \right] - \text{c.c.} \quad (\text{S74})$$

With the relations obtained in Eqs. (S65) to (S68) we have that $a_{R/L,j} \tilde{a}_{R/L,j} = |a_{R/L,j} \tilde{a}_{R/L,j}|$, and $b_{R/L,j} \tilde{b}_{R/L,j} = |b_{R/L,j} \tilde{b}_{R/L,j}| e^{i2\phi_{R/L}}$. Together with the results in Eq. (S70) we can simplify $\Upsilon_{L/R}(\phi)$ to be

$$\Upsilon_L(\phi) = -i\Gamma_1 e^{i\phi} - \text{c.c.} = \Gamma_1 \sin \phi, \\ \Upsilon_R(\phi) = -i\Gamma_1 e^{-i\phi} - \text{c.c.} = -\Gamma_1 \sin \phi,$$

and the effective coupling Hamiltonian for Majorana fermions at the same end takes the following form

$$H_{\text{eff}}^{(1)} = i\Gamma_1 \sin \phi (\gamma_L \tilde{\gamma}_L - \gamma_R \tilde{\gamma}_R). \quad (\text{S75})$$

The coupling constant Γ_1 is calculated by

$$\Gamma_1 = \Upsilon^2 |u_{L,N} \tilde{u}_{L,N}| \left[\sum_{j=1}^N |a_{R,j} \tilde{a}_{R,j}| \sum_k \frac{|\Delta_{s,R}|}{\mathcal{E}_R^2(\Delta_{s,R}; \Delta_{p,R}; k)} - \sum_{j=1}^N |b_{R,j}^* \tilde{b}_{R,j}^*| \sum_k \frac{|\Delta_{s,R}|}{\mathcal{E}_R^2(\Delta_{s,R}; \Delta_{p,R}; k)} \right]. \quad (\text{S76})$$

We have assumed the uniformity of the parameters in the left and right wires of the junction that $|\Delta_{s,L}| = |\Delta_{s,R}|$, $|\Delta_{p,L}| = |\Delta_{p,R}|$, and therefore $|u_{L,N} \tilde{u}_{L,N}| = |u_{R,1} \tilde{u}_{R,1}|$ and $\mathcal{E}_L(\Delta_{s,L}; \Delta_{p,L}; k) = \mathcal{E}_R(\Delta_{s,R}; \Delta_{p,R}; k)$. We note that this condition is typically satisfied in the realistic systems. It is clear that the Γ_1 -term vanishes when the s -wave pairing $\Delta_{s,L/R}$ is absent.

To this end, we combine $H^{(0)}$ and $H_{\text{eff}}^{(1)}$ to reach finally the effective Hamiltonian for a Josephson junction formed by DIII class topological superconductors that

$$H_{\text{eff}} = i\Gamma_0 \cos \frac{\phi}{2} (\gamma_L \gamma_R - \tilde{\gamma}_L \tilde{\gamma}_R) + i\Gamma_1 \sin \phi (\gamma_L \tilde{\gamma}_L - \gamma_R \tilde{\gamma}_R). \quad (\text{S77})$$

Note that if treating ϕ as a fixed parameter, the Γ_1 -term in the above formula breaks time-reversal symmetry, which also reflects that the leading-order contribution to the coupling between Majorana fermions at the same end ($i\gamma_j \tilde{\gamma}_j$) should come from the second-order perturbation in the tunneling process. Actually, the direct coupling between γ_j and $\tilde{\gamma}_j$ does not experience the phase difference across the junction and should preserve time-reversal symmetry. This is because a uniform pairing phase in one end of the junction can be removed by a constant gauge transformation. Therefore the coupling between Majorana fermions at the same end can only be induced by electron tunneling and the minimum requirement is to consider the second-order tunneling process. Furthermore, the system restores time-reversal symmetry at $\phi = m\pi$, which explains why the Γ_1 -term is proportional to $\sin \phi$, and has 2π periodicity.

B. Josephson current

The Hamiltonian (S77) can be block diagonalized by a constant transformation in the Majorana bases that $\gamma'_1 = \gamma_1 + \tilde{\gamma}_2$, $\gamma'_2 = \gamma_2 + \tilde{\gamma}_1$, and $\tilde{\gamma}'_{1,2} = \mathcal{T} \gamma'_{1,2} \mathcal{T}^{-1}$, which sends H_{eff} to be $H_{\text{eff}} = i(\Gamma_0 \cos \phi/2 + \Gamma_1 \sin \phi) \gamma'_1 \gamma'_2 - i(\Gamma_0 \cos \phi/2 - \Gamma_1 \sin \phi) \tilde{\gamma}'_1 \tilde{\gamma}'_2$. The Andreev bound state spectra are obtained by

$$E_{n_{f'}, \tilde{n}_{f'}}(\phi) = (\Gamma_0 \cos \phi/2 + \Gamma_1 \sin \phi)(2n_{f'} - 1) + (\Gamma_0 \cos \phi/2 - \Gamma_1 \sin \phi)(2\tilde{n}_{f'} - 1), \quad (\text{S78})$$

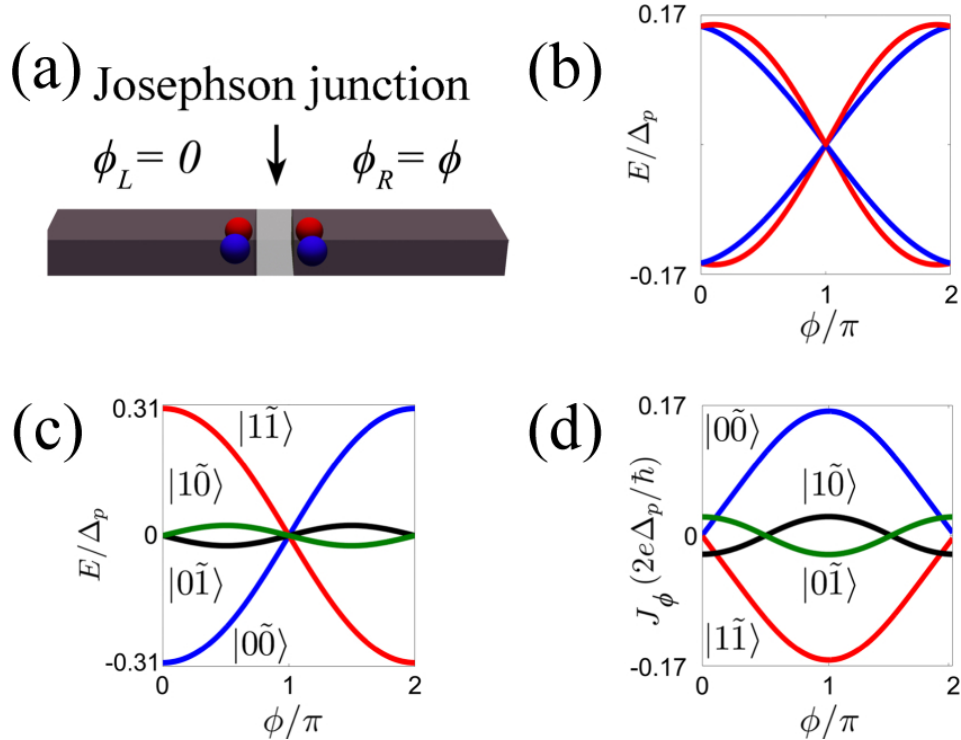


FIG. S4: Josephson effect in DIII class 1D topological superconductor with the inclusion of random disorder scattering. (a) The sketch of a Josephson junction with phase difference ϕ . (b) The single particle Andreev bound state spectra versus the phase difference ϕ . (c) The energy spectra of the four qubit states $|n_1 \tilde{n}_1\rangle$ ($n_1, \tilde{n}_1 = 0, 1$) according to the results in (b). (d) The Josephson currents (in units of $2e\Delta_p/\hbar$) for different topological qubit states. In the numerical simulation the amplitude of the random on-site disorder potential is set as $V_{\text{dis}} \sim 1.0\text{meV}$. Other parameters are taken that $\Delta_p = 1.0\text{meV}$, $\Delta_s = 0.25\text{meV}$, $E_{\text{so}} = 0.1\text{meV}$, the width of the junction $d = 0.75\xi$, and in middle trivial region (gray color) of the junction the chemical potential is set to be at the band bottom.

which are doubly degenerate at $\phi = m\pi$, reflecting the time-reversal symmetry at these points. Here $n_{f',\tilde{f}'}$ are complex fermion number operators for f and f' modes, respectively. The Josephson current then reads

$$J_\phi = \left(\frac{e\Gamma_0}{2\hbar} \sin \frac{\phi}{2} + \frac{e\Gamma_1}{2\hbar} \cos \phi\right)(2n_{f'} - 1) + \left(\frac{e\Gamma_0}{2\hbar} \sin \frac{\phi}{2} - \frac{e\Gamma_1}{2\hbar} \cos \phi\right)(2n_{\tilde{f}'} - 1). \quad (\text{S79})$$

The equation (S79) shows all the nontrivial results for the Josephson effect in a DIII class 1D topological superconductor. In particular, for the even parity states ($|0\tilde{0}\rangle$ and $|1\tilde{1}\rangle$) we have the Josephson currents that $J_\phi^{\text{even}} = \pm \frac{e}{\hbar} \Gamma_0 \sin \frac{\phi}{2}$, which are of 4π periodicity, while for the odd parity states ($|0\tilde{1}\rangle$ and $|1\tilde{0}\rangle$) the Josephson currents $J_\phi^{\text{odd}} = \pm \frac{e}{\hbar} \Gamma_1 \cos \phi$ exhibit 2π periodicity. The difference in the periodicity reflects different mechanisms for the Josephson currents J_ϕ^{even} and J_ϕ^{odd} . The currents J_ϕ^{even} for the even parity states are contributed from the Γ_0 -term in the effective coupling Hamiltonian, which is due to the direct coupling between Majorana modes at different ends of the junction. Therefore the currents J_ϕ^{even} are a consequence of the single-electron tunneling process and has 4π periodicity. On the other hand, as contributed from the Γ_1 term, the Josephson currents J_ϕ^{odd} are resulted from the second-order tunneling process which corresponds to the Cooper pair tunneling, therefore being of 2π periodicity. Furthermore, the currents J_ϕ^{odd} are nonzero even for $\phi = 0$, which reflects the fact that the odd-parity states violate time-reversal symmetry even H_{eff} preserves at $\phi = m\pi$.

The 4π periodicity of the Josephson currents for even parity states can also be understood in the following way. For the direct coupling between Majorana fermions at different ends, when the phase difference across the junction advances 2π , the coupling coefficients change only π phase and thus change sign. The generality of this argument implies that the 4π periodicity of J_ϕ^{even} is stable against the disorder scattering without breaking time-reversal symmetry. On the other hand, for odd parity states, the two-fold degeneracy at $\phi = m\pi$ is protected by time-reversal symmetry, which shows that the qualitative properties of the Josephson currents J_ϕ^{odd} are also stable against the TRI disorder scattering. The numerical results are shown in Fig. S4.

With the above results we find that in experiment there are several different ways to distinguish J_ϕ^{even} and J_ϕ^{odd} . For instance, one can measure the periodicity of the Josephson currents, or measure the currents at $\phi = \pi/2$ where $J_\phi^{\text{even}} = \pm \frac{e}{\sqrt{2}\hbar} \Gamma_0$ and $J_\phi^{\text{odd}} = 0$. Furthermore, the two qubit states with the same total parity are distinguished by the direction of the currents. The qualitative difference in the Josephson measurements provides direct detection of the four topological qubit states in experiment.

-
- [1] Turek, I., Drchal, V., Kudrnovsky, J., Sob, M. & Weinberger, P. Electronic Structure of Disordered Alloys, Surfaces and Interfaces (Kluwer, Boston, 1997).
 - [2] Qi, X. -L., Hughes, T. L., Raghu, S. & Zhang, S. -C. Time-Reversal-Invariant topological superconductors and superfluids in two and three dimensions. *Phys. Rev. Lett.* **102**, 187001 (2009).
 - [3] Ivanov, D. A. Non-Abelian statistics of half-quantum vortices in p-wave superconductors. *Phys. Rev. Lett.* **86**, 268-271 (2001).
 - [4] Alicea, J., Oreg, Y., Refael, G., von Oppen, F. & Fisher, M. P. A. Non-Abelian statistics and topological quantum information processing in 1D wire networks. *Nature Phys.* **7**, 412-417 (2011).
 - [5] Kitaev, A. Y. Unpaired Majorana fermions in quantum wires. *Phys.-Usp.* **44**, 131-136 (2001).
 - [6] Bennett, C. H., DiVincenzo, D. P., Smolin, J. A. & Wootters, W. K. Mixed-state entanglement and quantum error correction. *Phys. Rev. A* **54**, 3824-3851 (1996).
 - [7] Laflamme, R., Miquel, C., Paz, J.-P. & Zurek, W. H. Perfect Quantum Error Correcting Code. *Phys. Rev. Lett.* **77**, 198-201 (1996).
 - [8] Fu, L. & Kane, C. L. Superconducting proximity effect and Majorana fermions at the surface of a topological insulator. *Phys. Rev. Lett.* **100**, 096407 (2008).